Global Ecology and Conservation 64 (2025) e03982

Contents lists available at ScienceDirect

Global Ecology and Conservation

journal homepage: www.elsevier.com/locate/gecco

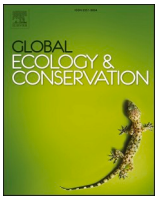

Original research article

Offshore wind farms can enhance the structural composition and functional dynamics of coastal waters

Liwei Si [a,b], Longfei Xu [a,b], Zhilin Wang [a,b], James R. Tweedley [c], Neil R. Loneragan [c], Yi Li [a,b], Hang Liu [a,b], Tao Tian [a,b,d], Zhongxin Wu [a,b,d,*]

[a] Center for Marine Ranching Engineering Science Research of Liaoning Province, Dalian Ocean University, Dalian, China
[b] College of Fisheries and Life Science, Dalian Ocean University, Dalian, China
[c] School of Environmental and Conservation Sciences and Harry Butler Institute, Murdoch University, Perth, Australia
[d] Key Laboratory of Environment Controlled Aquaculture, Ministry of Education, Dalian Ocean University, Dalian, China

ARTICLE INFO

Keywords:
Ecosystem function
Ecopath model
Renewable energy
Trophic flow
Trophic structure
Yellow Sea

ABSTRACT

Offshore wind farms (OWF) are rapidly emerging as essential infrastructure for transitioning to renewable energy, and this has been particularly important in the waters of China. To evaluate the impact of OWF construction, Ecopath models were developed for an OWF area and, separately, for a nearby control area, using biological and environmental survey data collected in 2022 and 2023. Functional groups were initially categorized into soft-substrate and hard-substrate (turbine monopiles) communities. The results showed that the colonization of turbine monopiles by sessile organisms significantly increased the productivity of most fish functional groups in the OWF area compared to the control. The OWF ecosystem exhibited higher trophic levels, especially for macroinvertebrates and fish, and a more complex food web with enhanced detritus flow than the control area. Mixed trophic impact analysis indicated a shift from a pelagic to a benthic-dominated system following OWF construction. Notably, detritus accounted for 52 % of total system throughput in the OWF area, compared to 38 % in the control area, highlighting a transition toward detritus-based energy flow. Furthermore, the OWF system showed significantly higher values for total system throughput, omnivory index, connectivity, Finn's cycling index, and ascendency. Overall, the presence of the OWF resulted in significant changes in the trophic flow and system structure, creating a more complex, mature, and stable benthic-dominated ecosystem. These findings indicate that the establishment of OWF enhances both the structural composition and functional dynamics of surrounding marine ecosystems.

1. Introduction

Offshore wind farms (OWF) are rapidly emerging as key infrastructure in the transition to renewable energy (Teilmann and Carstensen, 2012; Abramic et al., 2022). By 2023, global offshore wind capacity had reached 75.2 GW, representing a 24 % increase over the previous year due to 10.8 GW of capacity being installed (Global Wind Energy Council (GWEC), 2024). Moreover, this growth is predicted to continue and exceed the 380 GW target by 2030. China, is the global leader in offshore wind development, with a

* Corresponding author at: Center for Marine Ranching Engineering Science Research of Liaoning Province, Dalian Ocean University, Dalian, China.
E-mail address: wuzhongxin@dlou.edu.cn (Z. Wu).

https://doi.org/10.1016/j.gecco.2025.e03982
Received 6 August 2025; Received in revised form 4 November 2025; Accepted 19 November 2025
Available online 19 November 2025

cumulative offshore wind capacity of over 38 GW in 2023, ranking first worldwide and contributing over 50 % of global capacity (GWEC, 2024). While OWFs contribute significantly to clean energy production, they also bring notable physical, chemical, and biological changes to the surrounding marine environment (Zettler and Pollehne, 2006; Bailey et al., 2014). Growing attention has been directed toward the potential positive and negative impacts associated with OWFs, such as habitat modification, the spread of invasive species, changes to biodiversity and enhancement of commercial and recreational fishing (Gușatu et al., 2021, Watson et al., 2024).

The exploration, construction, operation, and decommissioning of OWF can induce temporary and permanent effects on marine ecosystems, including disruption of benthic habitats, seabed damage, and disturbances to species, such as fish, seabirds and marine mammals (Mueller-Blenkle et al., 2010; Shields and Payne, 2014). Construction activities can introduce additional stressors such as noise pollution, electromagnetic interference, and habitat fragmentation, further affecting benthic invertebrates, fish, and marine mammals (Lovich and Ennen, 2013; Premalatha et al., 2014). Conversely, OWF infrastructure, such as turbine monopiles and submarine cables, can provide new habitats for marine organisms, thereby altering local biodiversity (Lindeboom et al., 2011). These structures attract suspension-feeding organisms, increasing biomass and serving as a food source for species in higher trophic levels (Raoux et al., 2017). Studies report that over 95 % of the biomass surrounding turbine monopiles consists of suspension feeders that contribute to the processing of suspended particles (Coolen et al., 2020). The accumulation of detritus around these structures creates favorable conditions for sessile organisms, including deposit feeders (Leonhard and Pedersen, 2005). It has been estimated that a single turbine monopile can increase the biomass of sessile organisms by up to 4000 times compared to the original substrate (Rumes et al., 2013). Additionally, the gravel substrate surrounding the base of offshore turbine monopiles and detached organisms, such as mussels, offer predatory species additional foraging opportunities (Petersen and Malm, 2006). OWF can also act as refuges for fish, as turbine monopiles hinder trawling, and some OWFs are designated as no-fishing zones, improving habitat conditions for reproduction and survival (Gill et al., 2020).

This increase in biodiversity and biomass in areas with OWF, often referred to as the “reef effect,” is associated with enhanced habitat complexity (Petersen and Malm, 2006; Langhamer, 2012). Numerous authors have examined the reef effect across sessile organisms, soft substrate benthos, and benthic-pelagic fish communities, highlighting the potential ecological benefits of OWFs (e.g. Wilhelmsson and Malm, 2008; Leonhard et al., 2011). However, most previous studies focused primarily on the impacts of OWF on particular species e.g. seabirds, marine mammals and demersal fish and the overall community composition in OWF areas (Garthe et al., 2023; Lemasson et al., 2024; Bicknell et al., 2025). Additionally, the majority of these studies were conducted at the scale of individual turbines, with few assessing effects at the scale of entire OWFs. Given the substantial expansion of OWFs, understanding their impacts on whole food webs and ecosystem-level processes has become increasingly important (Yang et al., 2019; Watson et al., 2024).

Coastal ecosystems are increasingly subject to multiple anthropogenic pressures, including intensive fisheries, coastal aquaculture, and expanding offshore energy developments (e.g., Lozano-Montes et al., 2025). As OWFs become a prominent feature of coastal seascapes, understanding their interactions with existing human activities and ecosystem processes is essential for sustainable marine spatial planning. In recent years, increasing attention has been given to ecosystem-based approaches that comprehensively investigate the ecological consequences of offshore wind energy development. To this end, the efficacy of employing an ecosystem-based modeling framework to examine the potential consequences of OWF implementation in coastal waters has been explored. The Ecopath with Ecosim (EwE) software provides a powerful framework for analyzing ecosystem dynamics, material cycling, and energy flow through food webs (Christensen et al., 2005). The EwE framework has been extensively applied across both marine and freshwater ecosystems to enhance understanding of trophic interactions and to support effective fisheries and ecosystem-based management (Wu et al., 2016; Stock et al., 2023; Lozano-Montes et al., 2025).

In the context of offshore wind energy development, Raoux et al. (2017), (2019) constructed an Ecopath model to represent ecosystem conditions prior to wind farm installation and subsequently developed a dynamic Ecosim model to simulate the “reef effect” associated with the introduction of hard substrates from turbine foundations and scour protections. Their comparative analysis of network functioning and food web structure before and after construction revealed enhanced ecosystem maturity and increased biomass of benthic fish species in the post-construction phase. In contrast to earlier studies that primarily examined the ecological impacts of fixed-bottom offshore wind farms, Adge et al. (2024) were the first to apply the EwE framework to predict and quantify the ecosystem effects of floating OWFs, demonstrating that floating platforms can substantially alter local ecosystem structure and function. Similarly, Couce Montero et al. (2025) developed a high-resolution Ecospace model to assess the medium-term impacts of OWFs on food web dynamics and to identify potential spatial conflicts between ecological and human uses. However, despite these applications of ecosystem modelling to OWFs, most assessments have relied on simulated scenarios rather than empirical data collected after OWF construction (Pezy et al., 2020). A notable exception is the study by Wang et al. (2019), who developed an Ecopath model for the Rudong OWF in Jiangsu Province, China, using biological field data collected before construction and five years after operation. Their findings suggested that OWF development enhanced ecosystem maturity, functional efficiency, and recycling processes. Nevertheless, while this study incorporated valuable empirical observations, it did not fully capture several key ecological processes. In particular, the model omitted structural and biological components introduced by turbine foundations such as sessile organisms and reef-associated fish and their associated trophic linkages.

The Zhuanghe OWF in the North Yellow Sea was constructed between 2019 and 2021 and is the largest offshore wind project in northeast China, with an installed capacity of 1.35 GW and an annual output exceeding 3.3 billion kWh. Despite its commercial significance and large operational scale, the ecosystem-level effects of the Zhuanghe OWF have not yet been evaluated. We hypothesize that the introduction of additional hard substrates from OWF installations promotes the aggregation of benthic organisms and fish, thereby altering the regional biotic composition and trophic interactions. These changes are predicted to affect the overall structure

and function of coastal ecosystems compared with control areas without OWFs. To evaluate the potential ecosystem differences between OWF and similar areas without OWFs we developed two Ecopath models using biological and environmental survey data collected from the Zhuanghe OWF and a nearby control area without any OWF activity. Functional groups in each model were specifically and clearly categorized by habitat type, encompassing hard-substrate communities associated with turbine monopiles and soft-substrate communities present at both sites. By comparing ecosystem energy flows and structural characteristics between the two systems, we assessed the ecological impacts of OWF development on regional food webs and trophic dynamics. The results provide insights into how OWFs influence the structure and function of coastal ecosystems, offering guidance for marine habitat conservation and supporting the sustainable planning and development of future OWF projects.

2. Material and methods

2.1. Study area and data collection

The Zhuanghe OWF (39°26′~39°33′N, 123°9′~123°15′E), located in the eastern waters of Wangjia Island, Zhuanghe City, Liaoning Province, is the first project of its kind in Northeast China to be approved by the National Energy Administration. The Zhuanghe OWF II, a part of wind power project, covers approximately 48 km^2 in water depths ranging from 18 to 25 m (average depth: ~20 m), and contains 60 turbine monopiles, each with a capacity of 5 MW, for a total installed capacity of 300 MW (Fig. 1). Construction started in June 2019 and was substantially completed by September 2021. Each turbine monopile extends 20 m under the water surface and has a diameter of 7 m, providing approximately 440 m^2 of submerged surface area available for colonization by sessile organisms. Extensive oyster aquaculture rafts are located adjacent to the OWF, which could serve as a potential recruitment source for oysters and other sessile organisms colonizing the OWF. Moreover, this area is an important fishing ground in the northern Yellow Sea, serving as a key feeding and spawning habitat for ecologically and commercially valuable species, such as the Chinese white shrimp *Penaeus chinensis* and Small yellow croaker *Larimichthys polyactis* (Lin et al., 2013; Li et al., 2018). However, cumulative pressures from overfishing and climate variability have led to notable changes in species composition, biomass distribution, and trophic interactions within the ecosystem with a decline in catch rates of both *L. polyactis* and *P. chinensis* (Cui et al., 2024).

To evaluate the ecological effects of OWF construction, a control area (39°26′~39°33′N, 123°18′~123°24′E) was selected approximately 6 km east of the wind farm (Fig. 1). This area was matched to the OWF site in terms of environmental conditions, including substrate type, water depth, and geographic area. While the OWF area includes both soft substrate and artificial hard structures (i.e. turbine monopiles), the control area is characterized solely by soft substrate. Biological sampling focused on collecting data essential for Ecopath modelling, including biomass and dietary composition of key functional groups. Targeted functional groups included primary producers, suspended particulate organic matter, zooplankton, benthic invertebrates, and fish.

2.2. Ecopath model construction

2.2.1. Ecopath modelling approach

The Ecopath module of the EwE 6.6.8 software (Polovina, 1984; Christensen and Walters, 2004) was used to quantitatively assess the structural and functional dynamics of the OWF and control area. Ecopath models ecosystems as ecologically interconnected

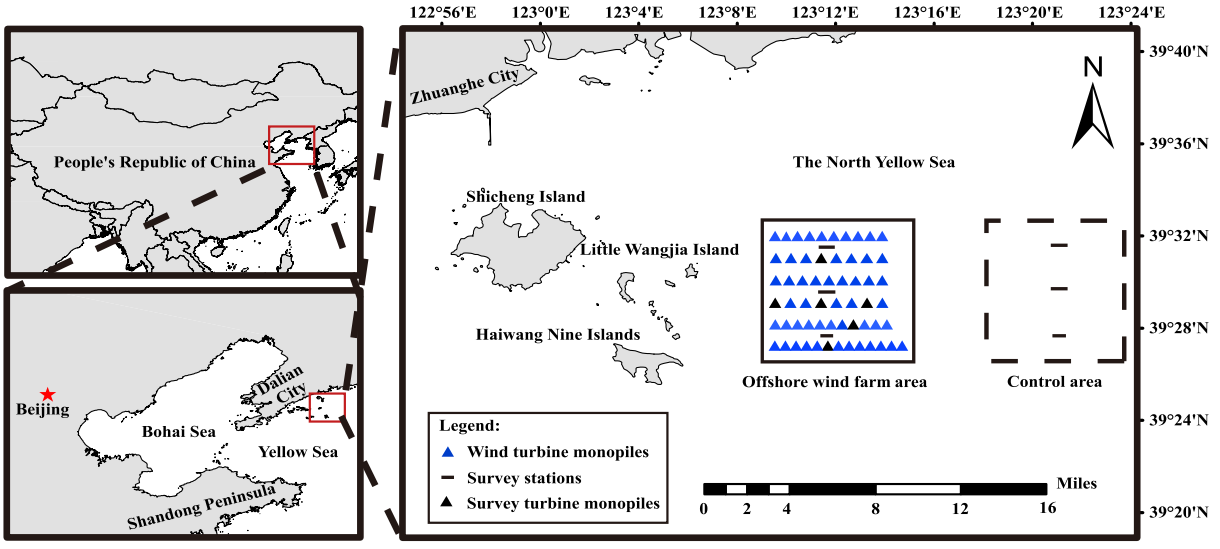

Fig. 1. Study area and location of the Zhuanghe offshore wind farm (OWF) and control area. Symbols denote the location of the sampling stations in the two areas in the northern Yellow Sea, China.

functional groups (Christensen and Walters, 2004). Based on the principle of energy conservation, the model assumes the ecosystem is in a steady state at any given time, where the energy input and output for each functional group are balanced (Christensen et al., 2005). The model relies on two key equations (Christensen and Pauly, 1992):

The first equation defines the production of each functional group as the sum of fishing mortality, predation mortality, net migration, biomass accumulation and other mortality, as detailed in Eq. (1):

$$B_i \cdot (\mathrm{P/B})_i \cdot EE_i - \sum_{j=1}^{n} B_j \cdot (\mathrm{Q/B})_j \cdot DC_{ji} - Y_i - E_i - BA_i = 0 \quad (1)$$

where B_i represents the biomass of functional group i, P_i denotes the production of functional group i, $(P/B)_i$ is the production to biomass ratio for functional group i, $(Q/B)_j$ is the consumption to biomass ratio for functional group j, EE_i indicates the ecotropic efficiency of functional group i, DC_{ij}, signifies the proportion of prey i in the diet of predator j, Y_i is the total catch of functional group i, E_i reflects the net migration rate (emigration minus immigration), and BA_i represents the biomass accumulation of functional group i.

The second equation describes the energy balance in a compartment, as shown in Eq. (2):

$$Q_i = P_i + R_i + U_i \quad (2)$$

The consumption rate of the i group (Q_i) is dictated by the mass balance requirement that it must equal the sum of the group's production (P_i), respiratory losses (R_i, gC m^{-2}), and excretion of unassimilated food (U_i).

Overall, B_i, Y_i, DC_{ij}, P/B, and Q/B for each functional group serve as model inputs, while EE is the output. All data in this study were standardized to a one-year timeframe, with biomass, production, and other energy flows expressed in terms of wet weight in tonnes. km^{-2}.

Table 1
Summary of the input data and output parameters estimated by the Ecopath model of the Zhuanghe offshore wind farm (OWF) and control area (Control) in the northern Yellow Sea, China. Note that some functional groups only occur in the OWF.

No.	Functional group	TL		B		*P/B*		*Q/B*		*EE*	
		OWF	Control	OWF	Control	OWF	Control	OWF	Control	OWF	Control
1	Zooplanktivorous fish	**2.86**	**2.86**	2.89	2.28	2.37	2.37	7.98	7.98	**0.89**	**0.83**
2	Piscivorous fish	**3.55**	**3.53**	0.57	0.45	3.06	3.06	11.10	11.10	**0.47**	**0.33**
3	*Scomberomorus niphonius*	**3.87**	**3.80**	0.25	0.18	1.01	1.01	7.20	7.20	**0.25**	**0.23**
4	*Hexagrammos otakii*	**3.68**	**3.65**	0.34	0.14	1.74	1.74	9.20	9.20	**0.28**	**0.26**
5	*Sebastes schlegelii*	**4.09**	**3.95**	0.46	0.15	2.24	2.24	9.90	9.90	**0.18**	**0.13**
6	*Thamnaconus modestus*	**3.33**	**3.30**	0.23	0.13	1.05	1.05	5.50	5.50	**0.37**	**0.18**
7	Gobiidae	**3.32**	**3.24**	2.49	1.06	1.46	1.46	6.50	6.50	**0.79**	**0.68**
8	*Larimichthys polyactis*	**3.72**	**3.57**	0.42	0.20	1.53	1.53	5.90	5.90	**0.73**	**0.72**
9	Demersal forage fish	**3.14**	**2.96**	2.00	1.09	3.43	3.43	18.90	18.90	**0.78**	**0.57**
10	Other demersal fishes	**3.92**	**3.79**	2.40	1.01	2.32	2.32	8.00	8.00	**0.77**	**0.72**
11	*Charybdis japonica*	**3.21**	**3.04**	1.26	0.79	3.20	3.20	11.30	11.30	**0.16**	**0.12**
12	*Rapana venosa*	**2.80**	**2.76**	3.38	1.00	9.18	9.18	30.90	30.90	**0.12**	**0.11**
13	*Mytilus edulis* on the surface of turbine monopiles	**2.00**	-	7.81	-	7.00	-	27.00	-	**0.94**	-
14	Bivalves on the surface of turbine monopiles	**2.00**	-	11.24	-	7.00	-	27.00	-	**0.95**	-
15	Echinoderms on the surface of turbine monopiles	**2.00**	-	4.19	-	1.30	-	5.90	-	**0.97**	-
16	Crustaceans on the surface of turbine monopiles	**2.31**	-	4.15	-	7.13	-	24.11	-	**0.89**	-
17	Polychaetes on the surface of turbine monopiles	**2.00**	-	5.18	-	6.80	-	25.72	-	**0.91**	-
18	Gastropods on the surface of turbine monopiles	**2.07**	-	1.55	-	8.50	-	28.30	-	**0.83**	-
19	Other sessile organisms on the surface of turbine monopiles	**2.05**	-	2.88	-	8.50	-	28.30	-	**0.89**	-
20	Cephalopods	**3.60**	**3.04**	1.25	0.60	3.30	3.20	11.00	11.30	**0.61**	**0.12**
21	Soft substrate crabs	**2.91**	**2.86**	1.64	1.24	8.30	8.30	28.31	28.31	**0.71**	**0.70**
22	Other soft substrate crustaceans	**2.82**	**2.74**	3.17	2.30	6.90	6.90	28.00	28.00	**0.76**	**0.72**
23	Soft substrate gastropods	**2.12**	-	1.13	-	9.50	-	32.30	-	**0.36**	-
24	Other soft substrate organisms	-	**2.12**	-	5.99	-	10.50	-	35.30	-	**0.94**
25	Zooplankton	**2.05**	**2.05**	15.68	14.26	25.00	25.00	122.10	122.10	**0.47**	**0.51**
26	Phytoplankton	**1.00**	**1.00**	25.43	20.52	106.52	106.52	-	-	**0.43**	**0.59**
27	Detritus	**1.00**	**1.00**	86.00	42.00	-	-	-	-	**0.65**	**0.39**
	Medians	2.84	3.04	2.445	1.01	3.43	3.13	15.1	11.1	0.72	0.54
	Mean value weighted by biomass	2.38	2.44	7.23	5.02	18.38	27.89	17.19	22.68	0.65	0.51

TL: trophic level; B: Biomass ($t \cdot km^{-2} \cdot y^{-1}$); *P/B*: production/biomass; *Q/B*; consumption/biomass; *EE*: ecotrophic efficiency; non-bold: input; bold: output; —: not present

2.2.2. Definition of functional groups

Based on field surveys and the literature, species of economic and ecological importance within the food webs of the two study areas were categorized into distinct functional groups. The ecosystem model of the Zhuanghe OWF area comprises 26 functional groups, while the control area includes 19 functional groups, effectively covering the full energy flow dynamics of both ecosystems (see Table 1 and Table S1 for a full list of functional groups). The difference in the number of functional groups between the OWF and control area reflects the presence of additional taxa in the OWF area that were absent from the control area. Notably, the OWF area supports sessile organisms, facilitated by the rough surfaces of turbine monopiles, which promote colonization and community development. These sessile communities provide essential food resources and habitat for other species, contributing to the distinct ecological dynamics of the OWF system. To better reflect habitat-specific community composition, functional groups were first classified according to substrate type: hard substrate (e.g. bivalves, crustaceans and gastropods on the surface of turbine monopiles) and soft substrate (e.g. crabs, other crustaceans and gastropods). Due to its considerable biomass and ecological influence, the blue mussel *Mytilus edulis,* found only on the surface of turbine monopiles, was categorized as a distinct functional group. Seven single-species functional groups were established for commercially and recreationally important fishery species in both areas: five for teleosts, i.e. Korean rockfish *Sebastes schlegeli*, Fat greenling *Hexagrammos otakii*, Black scraper *Thamnaconus modestus*, Japanese Spanish mackerel *Scomberomorus niphonius*, and Small yellow croaker *Larimichthys polyactis*, and two invertebrates, i.e. – the gastropod Purple whelk *Rapana venosa* and the crustacean Japanese swimming crab *Charybdis japonica*. The remaining species were aggregated into broader functional groups based on shared life history traits, feeding strategies, and habitat characteristics, such as zooplanktivorous fish, piscivorous fish, other demersal fishes, and cephalopods. A detailed list of the functional groups in the Ecopath model is presented in Table S1.

2.2.3. Parameterization of Ecopath model

In this study, biological analysis and assessment were conducted based on survey data from field observations, published information, and empirical equations. The biomass inputs for macroinvertebrates and fish in the Ecopath models were primarily derived from resource survey data. In the OWF area, the biomass of organisms on the surface of turbine monopiles were collected and estimated by using 0.25 × 0.25 m quadrats by SCUBA diving, with five replicates at each station seasonally. The biomass of fish and macroinvertebrates in the study area was estimated using single bottom trawl surveys, with three parallel transects established between each row of turbine monopiles to ensure representative coverage. In the control area, three parallel trawl stations were randomly selected for sampling. The otter trawl net had a mouth opening of 10 m, a codend length of 20 m and was constructed of 20 mm stretch mesh in the codend. Trawls were towed for 60 min duration over a transect length of 5.5 km and covered a swept area of 0.05 km^2 at each station. In both areas, three replicate macrobenthos samples were collected using a 0.05 m^2 box sampler at each of the three sampling stations. Samples were sieved through a 0.5-mm mesh for biomass analysis. The plankton samples were collected using vertical tow from 2 m above the bottom to the surface at a speed of 0.5 m/s by plankton nets (zooplankton, type II, 0.160 mm mesh size, 316 mm mouth diameter; phytoplankton, type III, 0.077 mm mesh size, 370 mm mouth diameter). Three replicated tows were completed with each net at each station. Phytoplankton biomass was quantified by measuring chlorophyll *a* with a fluorometer (Turner Designs, USA), with chlorophyll *a* concentration standardized to biomass estimates (Ning et al., 1995; Wang et al., 1998).

Detritus biomass was calculated using the linear model proposed by Pauly et al. (1993), as follows:

$$\lg D = -2.41 + 0.954 \lg PP + 0.863 \lg E \tag{3}$$

where D [g(C)/m^2] is detritus biomass, PP [g(C)/(m^2·a)] is the primary production, and E (m) is the euphotic depth.

The production to biomass (P/B) ratio for fish represents the instantaneous total mortality rate (Z), encompassing both fishing and natural mortality (Pauly, 1980). The consumption to biomass (Q/B) ratio was determined using the tail-fin profile ratio regression model (Palomares and Pauly, 1998), and P/B and Q/B ratios for other functional groups were sourced from literature on similar local and adjacent marine ecosystems (Wu et al., 2016; Liu et al., 2019).

The dietary composition matrix for the Ecopath model was constructed using data from relevant published studies and stomach content analyses conducted in both the OWF and control areas. Stomach content analysis were conducted for key species, i.e. *H. otakii* (n = 65) and *Sebastes schlegelii* (n = 54) and other demersal fishes (n = 30), zooplanktivorous fishes (n = 30), piscivorous fishes (n = 30). Samples of fish collected during spring (May) and autumn (August) of 2023 and 2024 were used for stomach content analyses. Dietary information for other macrobenthic and sessile organisms was sourced from comparable studies in other regions (Yang, 2001; Liu et al., 2020).

Due to restrictions on commercial fishing within the OWF area, recreational fisheries constitute the primary fishing activity. We used the most recent available recreational catch data from 2022 and 2023, obtained from field surveys and the China Fishery Statistical Yearbook (Cheng, 2004; MARA-BF, 2023, 2024), to estimate catches of targeted species in the area (e.g. *S. schlegeli*, *H. otakii* and *S. niphonius*). In the control area, commercial fishing included both single- and double-boat trawling. Catch inputs for the model were based on average total landings from 2022 to 2023 (Cheng, 2004; MARA-BF, 2023, 2024).

The Pedigree Index was calculated to evaluate the uncertainty and overall reliability of the Ecopath model input parameters with high values indicating more data come from the local area (Christensen and Walters, 2004). Pre-balancing (PREBAL) diagnostic analysis (Link, 2010) was then conducted to assess the adequacy of the input data prior to model balancing. Subsequently, the models were balanced in accordance with established thermodynamic and ecological principles. A detailed description of data quality assessment and model balancing procedures is provided in the supplementary material. (Supplementary File 1).

2.3. Ecosystem structure analysis

The impacts of OWF on marine ecosystem structure and function were assessed utilizing indicators from the ecological network analysis (ENA) routine in Ecopath. This routine calculates metrics that characterize the ecosystem structure including trophic levels (TL), Mixed Trophic Impact (MTI), and keystone species for each functional group within the food web. The MTI analysis also evaluates the relative impact of a slight increase in biomass (up to 10%) of one functional group on others, revealing both direct predator-prey

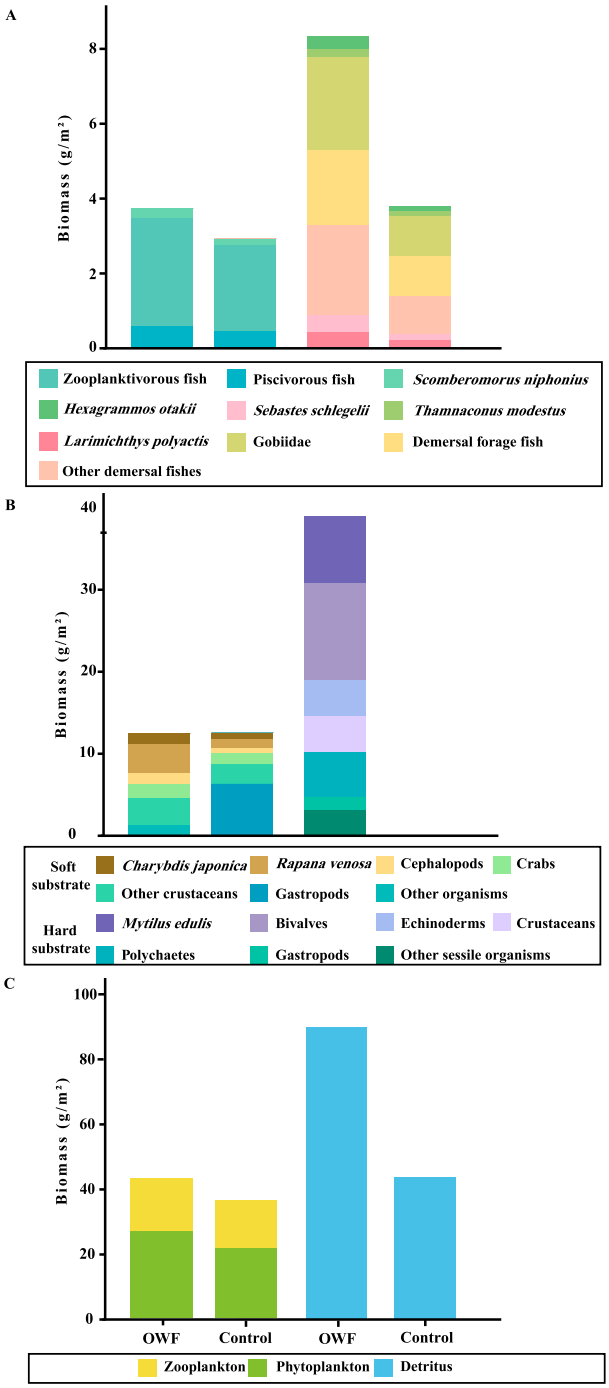

Fig. 2. The biomass of (A) pelagic fish and bottom fish, (B) soft substrate and hard substrate organisms and (C) plankton and detritus in the Zhuanghe offshore windfarm (OWF) and the control area (Control) in the northern Yellow Sea, China. Note, no hard substrate species were found in the Control area.

interactions and indirect cascading effects on competitors (Ulanowicz and Puccia, 1990). Keystone species were identified based on the magnitude of their effects and lower biomass proportions within functional groups, following the criteria proposed by Libralato et al. (2006). Specifically, the keystone index was calculated by integrating the relative total MTI and the inverse of biomass, enabling species that play critical roles in maintaining ecosystem structure and function despite their low abundance to be identified. These analyses provided insights into the cascading ecological consequences of OWF development and allowed for a more comprehensive evaluation of shifts in food web dynamics after the construction of the OWF.

2.4. Ecosystem Functioning Analysis

Ecological Network Analysis indices also describe the energy flow, trophic structure, system scale, maturity, and stability in ecosystems (Christensen and Walters, 2004). Among these indices, Total System Throughput (TST) serves as a fundamental indicator of ecosystem size and activity, reflecting the total flow of energy or matter within the system and providing a measure of its overall scale and developmental maturity (Christensen et al., 2005). Several key ratios offer further insights into ecosystem development and energetics. The total primary production to total respiration ratio (TPP/TR), the total biomass to total throughput ratio (TB/TT), and

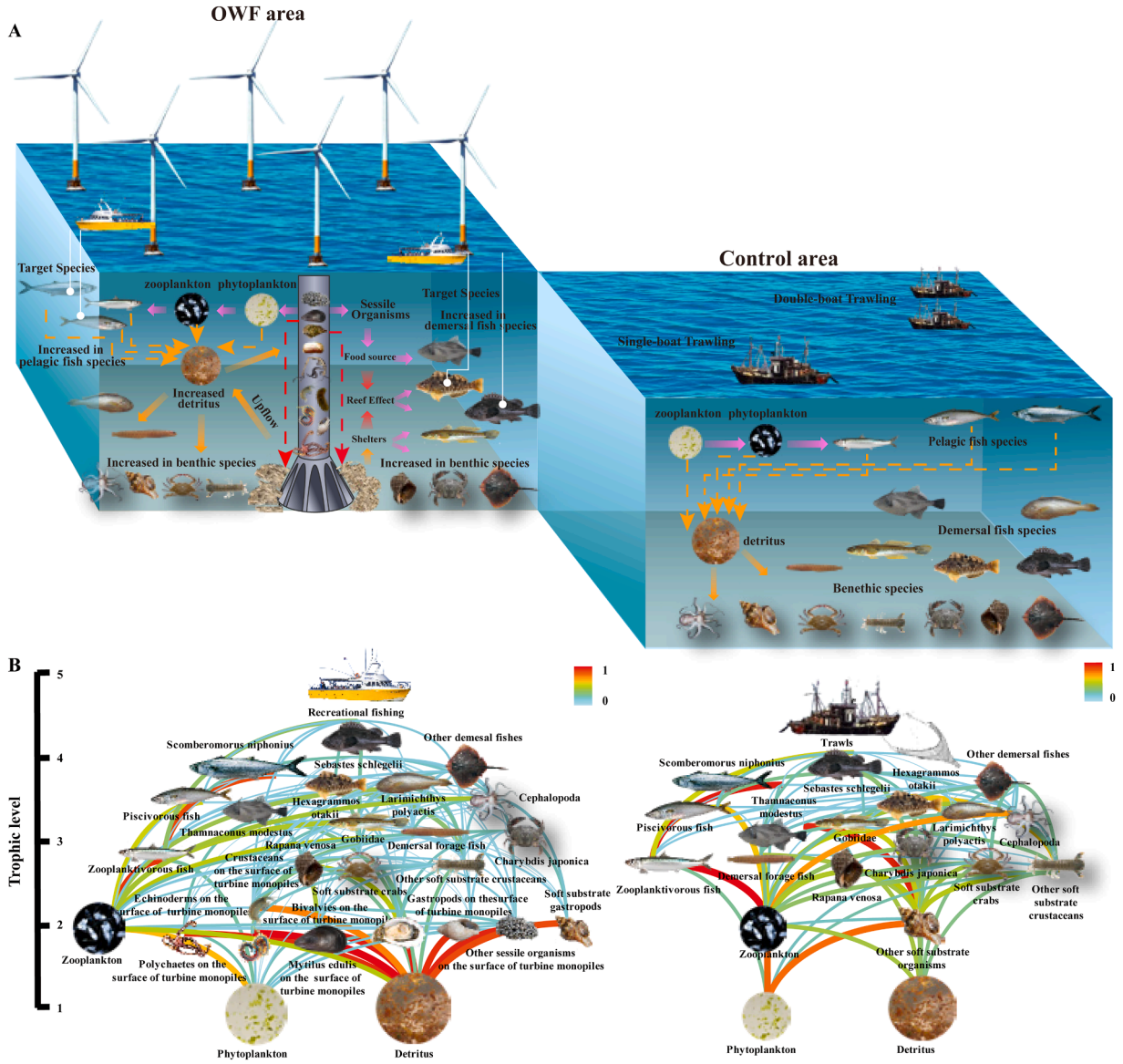

Fig. 3. (A) Ecological process model and (B) flow diagrams estimated by Ecopath models (B) in Zhuanghe offshore wind farm (OWF) and control area in the northern Yellow Sea, China. Lines in the flow diagram represent the energy transfer process, and the colour indicates the proportion that prey contributes to a predator's diet from least flow in blue to greatest flow in red.

the total primary production to total biomass ratio (TPP/TB) are used to evaluate system maturity and energy efficiency, consistent with thermodynamic and entropy-based principles proposed by Odum (1969). Food web complexity is assessed through the connectance index (CI) and the system omnivory index (SOI). Higher values for both CI and SOI indicate a greater degree of trophic interconnectivity and system maturity (Pauly et al., 1993). In addition, Finn's cycling index (FCI) quantifies the proportion of energy or material that is recycled within the system, while Finn's mean path length (FML) represents the average number of trophic links energy passes through before leaving the system—both are considered as indicators of system maturity and resilience (Finn, 1976). The ascendency (A) metric reflects the level of organization and flow control among trophic interactions, and is interpreted as a measure of the system's developmental stage and stability (Christensen et al., 2005). Finally, the transfer efficiency (TE) describes the proportion of energy transferred from one trophic level to the next, and is often visualized through a Lindeman spine plot, which linearizes food web structure to display energy transfer efficiency, biomass dissipation to detritus, and trophic flow patterns across trophic levels (Lindeman, 1942).

3. Results

3.1. Comparison of ecosystem structure

3.1.1. Food web characteristics

The TL of functional groups in the OWF area ranged from 1.00 to 4.09, whereas in the control area it ranged from 1.00 to 3.95 (Table 1). The average TL in the OWF area (2.38) was slightly lower than that in the control area (2.44), indicating a community structure more concentrated in lower TL. *Sebastes schlegelii* was the top predator in both areas, with a trophic level of 4.09 in the OWF area and 3.95 in the control. TLs for benthic invertebrates and zooplankton in both regions ranged from 2.00 to 3.60. Notably, the economically valuable species *S. niphonius* had TLs of 3.87 (OWF) and 3.80 (control), while *C. japonica* had a TL of 3.21 and 3.04, respectively, indicating slightly higher trophic positions for these species in the OWF area than in the control area.

In both areas, over 80 % of the total biomass was concentrated in TLs < 2.5, primarily consisting of primary producers, suspension-feeders, herbivores, and invertebrates (Table 1). Within the OWF area, sessile organisms such as *M. edulis*, the Pacific oyster *Crassostrea gigas,* and associated invertebrates colonizing turbine monopiles accounted for approximately 49 % (37 $t.km^{-2}$) of the total system biomass (excluding primary producers and detritus) (Fig. 2), underscoring the ecological importance of these mid- to low-trophic level groups. Demersal fishes were also more abundant in the OWF area, with over two times the biomass (8.33 $t{\cdot}km^{-2}{\cdot}y^{-1}$) than in the control (3.8 $t.km^{-2}{\cdot}y^{-1}$). In contrast, the biomass of soft substrate organisms was ~12 $t.km^{-2}{\cdot}y^{-1}$ in both areas (Fig. 2). In the OWF area, the biomass of phytoplankton (25.43 $t.km^{-2}{\cdot}y^{-1}$) and detritus (86 $t.km^{-2}y^{-1}$) were higher than the control area (phytoplankton=20.52 $t.km^{-2}y^{-1}$, detritus=42 $t.km^{-2}{\cdot}y^{-1}$).

The ecotrophic efficiency (EE) values were generally higher in the OWF area for key species. Specifically, the EE values for the fish *S. schlegelii*, *H. otakii*, and *S. niphonius* in the OWF area were 0.18, 0.28, and 0.25, respectively, compared to 0.13, 0.26, and 0.23 in the control. For the gastropod *R. venosa* and portunid *C. japonica*, EE in the OWF area was 0.12 and 0.13, respectively, with EEs of 0.11 and 0.12 in the control. The EE of the bivalve *M. edulis* and other sessile organisms in the OWF area that were not present in the control exceeded 0.9, reflecting their substantial role in trophic energy transfer. Overall, both EE and biomass were higher in the OWF area, particularly among invertebrates and lower TL functional groups. The overall mean EE (0.65) and biomass (7.23 $t{\cdot}km^{-2}{\cdot}y^{-1}$) in the OWF area, excluding primary producers and detritus were greater by > 20 % than in the control area (0.51, 5.02 $t{\cdot}km^{-2}{\cdot}y^{-1}$) (Table 1, Fig. 2).

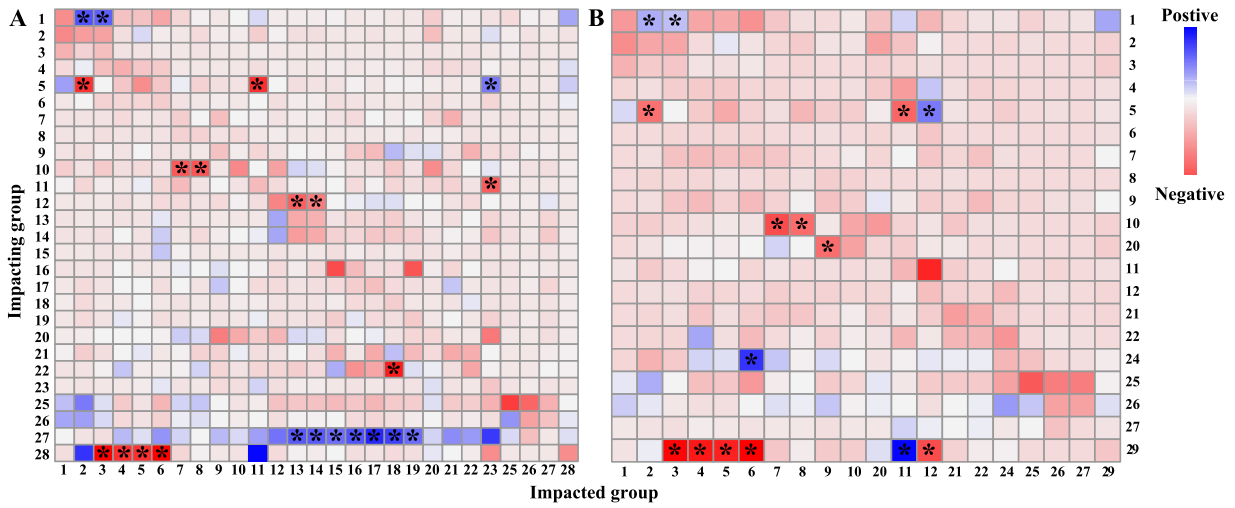

Fig. 4. Mixed trophic impact estimated by Ecopath (A) for Zhuanghe offshore wind farm and (B) control areas in northern Yellow Sea, China. The numbers 1–27 correspond to the functional groups listed in Table 1; 28 = recreational fishing; 29 = trawling.

Based on a comprehensive analysis of biological community composition, fishing activities, sediment characteristics, utilization patterns, and energy flow dynamics, comparative ecosystem models for both the OWF and control areas were constructed (Fig. 3 A). The structure of OWF and control area, predator-prey relationships and energy flow are represented in Fig. 3B. In both regions, primary producers and detritus constituted the foundational energy sources, serving as the principal drivers of ecosystem productivity.

3.1.2. *Mixed trophic impact and keystone index analyses*

The MTI analysis revealed that detritus and phytoplankton exert broadly positive effects across most functional groups,

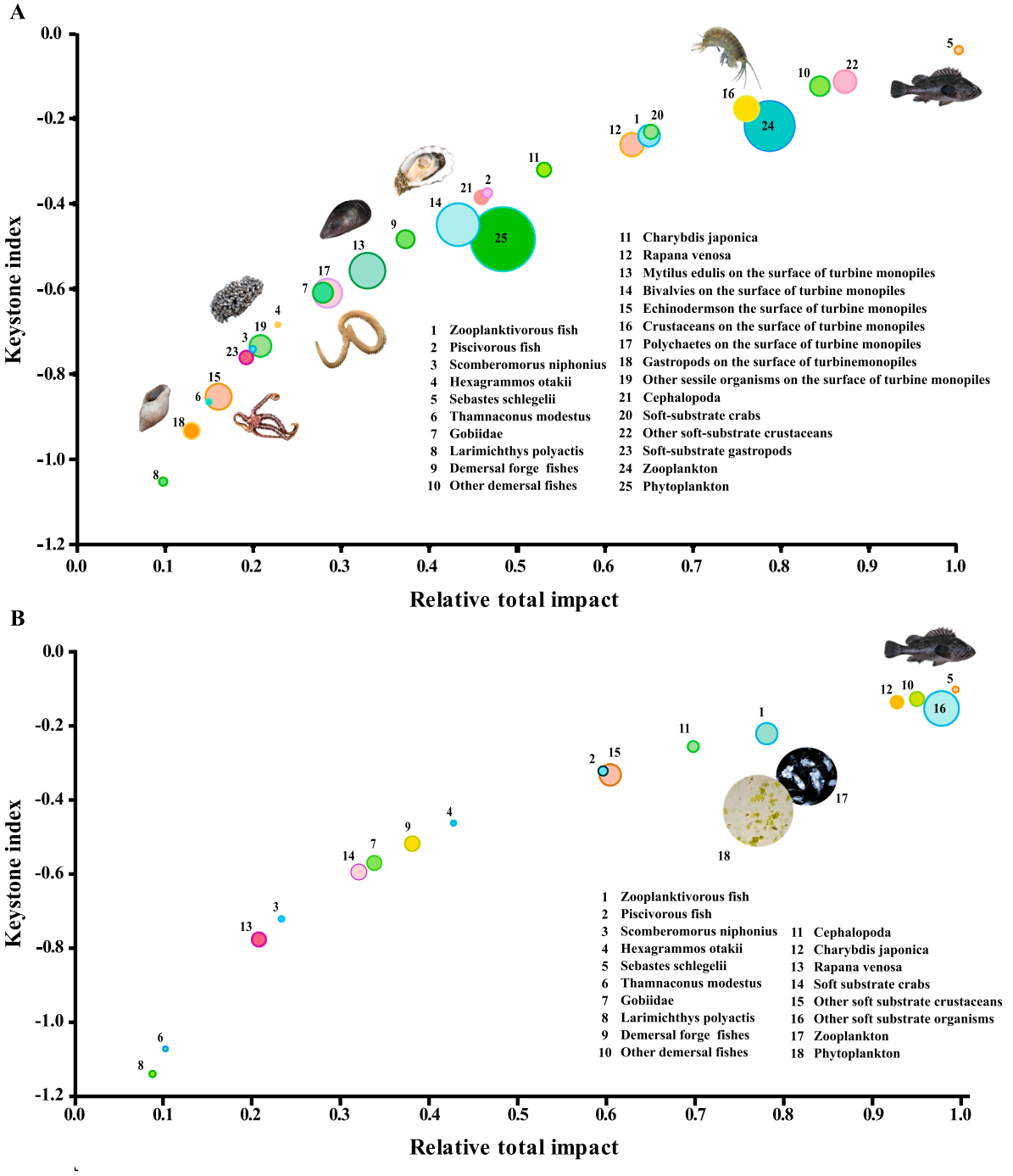

Fig. 5. Keystone index (Libralato et al. 2006) and relative total impact of each functional group for (A) Zhuanghe OWF and (B) control area in the northern Yellow Sea estimated by Ecopath. Circle size shows the percentage relative biomass of each group.

underscoring their roles as the foundational energy sources in both ecosystems (Fig. 4). Fishing activities had uniformly negative impacts on all harvested groups, with recreational fishing prevailing in the OWF area and commercial trawling dominant in the control area. These anthropogenic pressures, through trophic cascades, led to reduced biomass of target fish species, while indirectly benefiting zooplankton and other invertebrates due to predator release effects (Fig. 4). In the OWF area, *H. otakii* was negatively influenced by *S. schlegelii*. Zooplankton adversely affected sessile organisms on turbine monopiles, including *M. edulis*, other bivalves, and other sessile organisms. Each functional group also had a negative impact on its own population (i.e. through intraspecific competition) (Fig. 4A). In the control ecosystem, *S. schlegelii* and *H. otakii* negatively influenced *C. japonica*, and cephalopods affected demersal forage fish (Fig. 4B). Conversely, zooplanktivorous fish positively impacted piscivorous fish and *S. niphonius*.

In the OWF area, *S. schlegelii* had the highest value of keystone index value (-0.04) and highest relative total impact (1.00), followed by the "other soft substrate crustaceans" functional group (keystone index =-0.115, relative total impact = 0.872) (Fig. 5A). In the control area, *S. schlegelii* also had the highest keystone index (-0.0828) and relative total impact (1.00), followed by other demersal fishes (-0.109 and 0.956) and the decapod *C. japonica* (-0.118 and 0.52) (Fig. 5B). The relative total impact and keystone index for *S. schlegelii* and most high trophic level benthic fishes were greater in the OWF than the control area (Fig. 5).

3.2. Comparison of ecosystem function

3.2.1. Characteristics of ecosystem energy flows

In the OWF ecosystem, detritus accounted for 52 % of the total system flux, while primary producers contributed 48 %. In contrast, detritus represented only 38 % of the total system flux in the control ecosystem, with primary producers constituting 62 %. Network analysis was used to calculate the throughput of functional groups along a Lindeman spine, aggregated into five integrated TLs (Table 2, Fig. 6). In the OWF area, the most significant energy transfer efficiency occurs between TLs II and III (15.94 %). The overall energy transfer efficiency for the OWF area was 12.62 %, with the primary producer transfer efficiency at 11.07 % and the detritus transfer efficiency at 13.54 % (Table 2). In the control area, detritus's highest energy transfer efficiency occurred between trophic levels II and III (14.02 %). The total energy transfer efficiency of the system was 9.72 %, with 9.77 % attributed to producers and 9.62 % to detritus (Table 2).

The energy transfer between trophic levels in both the OWF and control area gradually declined in material flux as trophic levels increased (Fig. 6). The estimated total primary production in the OWF area was 2709 $t{\cdot}km^{-2}$, with 1170 $t{\cdot}km^{-2}$ allocated to trophic level II (Fig. 6). The total energy inflow to detritus was 2466 $t{\cdot}km^{-2}$, with 1539 $t{\cdot}km^{-2}$ coming from primary producers. In the control area, the total primary production was 2185.4 $t{\cdot}km^{-2}$ (19.33 % lower than the OWF), with 1287 $t{\cdot}km^{-2}$ of energy transferred to trophic level II. The total energy flowing into detritus was 1534 $t{\cdot}km^{-2}$ (37.8 % lower than OWF), with 898.4 $t{\cdot}km^{-2}$ originating from primary producers (Fig. 6).

3.2.2. General ecosystem characterization

The TST was greater by 42 % for the OWF area (8406.46 $t{\cdot}km^{-2}{\cdot}y^{-1}$) than the control area (5883.14 $t{\cdot}km^{-2}{\cdot}y^{-1}$), and the total system production was also greater by 30 % in the OWF (3454.85 vs 2660.61 $t{\cdot}km^{-2}{\cdot}y^{-1}$), indicating a larger system scale in the OWF area (Table 3). The TPP/TR was lower in the OWF area (1.47) than the control area (1.74). Conversely, the TPP/ TB ratio was approximately two times higher in the OWF area (40.95) than the control (20.56), while the TB/TST ratio (0.012) was similar in both areas (Table 3). These results indicate that the biomass in the OWF ecosystem is lower, but the system is at a more advanced stage of maturity than in the control area. The mean TL of the recreational fishing catch in the OWF area (3.52) was higher than in the control area (3.18). This index combined with the value of the gross efficiency of the fishery, reflects the importance of high TL species in the recreational landings from the OWF. The complexity of the food web, reflected in the CI (0.282) and SOI (0.231), being higher in the OWF area than the control area (0.279 and 0.215, respectively). The FCI(10.44) and MPL(3.103) in the OWF area also exceeded those of the control area (FCI=8.4, MPL=2.692), suggesting a higher level of nutrient cycling. The ascendency values were 8401 $t{\cdot}km^{-2}{\cdot}y^{-1}$ for the OWF area and 5486 $t{\cdot}km^{-2}{\cdot}y^{-1}$ for the control area, indicating that the OWF area is a more self-organizing system. Additionally, the Shannon diversity index in the OWF area (2.577) was greater than in the control area (1.869).

The Zhuanghe OWF ecosystem had a higher TST value compared to other OWF ecosystems, such as Seine Bay OWF, Gruissan coast, and Dieppe-Le Tré OWF (both in north-western France, but lower than the Rudong OWF (9232 $t{\cdot}km^{-2}{\cdot}y^{-1}$) in the East China Sea

Table 2
Transfer efficiency between different trophic levels of the Zhuanghe OWF and control area in the northern Yellow Sea, China. TL = Trophic level.

Sources	Offshore wind farm area (TL)				Control area (TL)			
	II	III	IV	V	II	III	IV	V
Producer	6.70 %	15.94 %	12.70 %	11.75 %	8.15 %	13.99 %	8.17 %	6.69 %
Detritus	14.47 %	13.01 %	13.19 %	12.12 %	7.78 %	14.02 %	8.168	6.70 %
All flows	11.19 %	13.75 %	13.05 %	12.01 %	8.03 %	14.00 %	8.17 %	6.69 %
Proportion of total flow originating from detritus	52 %				38 %			
Transfer efficiencies (calculated as geometric mean for TLII-IV)								
Transfer efficiency from primary producers	11.07 %				9.77 %			
Transfer efficiency from detritus	13.54 %				9.62 %			
Total energy transfer efficiency	12.62 %				9.72 %			

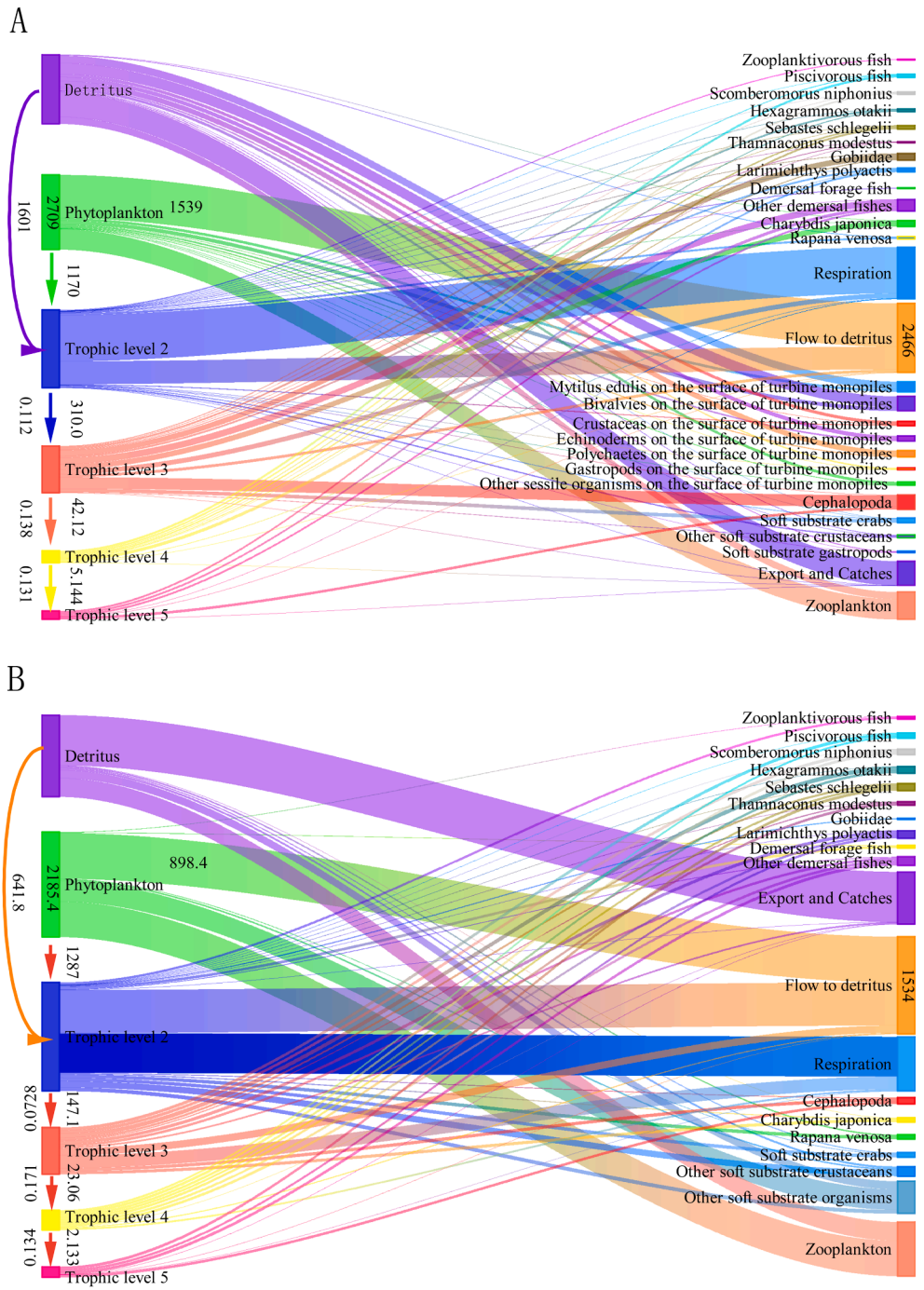

Fig. 6. Energy flow of discrete trophic levels for (A) the Zhuanghe offshore windfarm and (B) the control area in the northern Yellow Sea, China. The value on the right side (t·km^{-2}) of the arrow reflects the flow consumed by the next trophic level, and that on the left is the transfer efficiency (TE, %) between them.

(Table 3). The TST of Zhuanghe OWF was second only to the Bohai Sea (10074.2 t·km^{-2}·y^{-1}) (Table 3). Of the values for TPP/TR, TPP/TB, TB/TST, net system production, and calculated total net primary production, the Zhuanghe OWF were intermediate compared with other OWF systems (Table 3), suggesting that it is a relatively immature system in the early stages of development. The mean TL of the catch in the Zhuanghe OWF ecosystem (3.52) was second only to that of Fuerteventura in the Atlantic off north Africa and Lanzarote OWF area in the Canary Islands (3.57), and greater than the Bohai Sea (2.99) and Biscay Bay, south-western France (3.37). The values of CI and SOI indices for the Zhuanghe OWF ecosystem (0.282 and 0.231, respectively) were similar in magnitude to Seine Bay OWF

Table 3
Summary of the ecosystem attributes of the Zhuanghe OWF and control area estimated by the Ecopath model compared with offshore ecosystems and other OWF ecosystems. The largest value in each row is in bold typeface.

System statistics	OWF area[1] this study	Control area[1] this study	Yellow Sea[2] China	Bohai Sea[3] China	Rudong[4] China	Biscay bay[5] Spain	Madeira[6] Portugal	Seine Bay[7] France	Dieppe-Le Tre[8] France	Gruissan Coast[9] France	Fuerteventuraand Lanzarote islands[10] Spain	Units
Latitude and longitude	39°30′ N 123°12′ E	39°30′ N 123°22′ E	36°19′ N 123°17′ E	39°10′ N 120°05′ E	32°55′ N 121°21′ E	43°10′ N 1°25′ W	32°50′ N 17°16′ W	49°20′ N 0°15′ W	50°05′ N 1°10′ E	42°55′ N 3°20′ E	42°48′ N 3°02′ E	
Sum of all consumption	**3232.04**	2163.06	1954.97	691.43	2859	2312.3	823.52	-	-	-	1977.72	$t{\cdot}km^{-2}{\cdot}y^{-1}$
Sum of all exports	865.96	930.15	544.15	**4406.19**	1573	1058.11	866.32	-	-	-	547.79	$t{\cdot}km^{-2}{\cdot}y^{-1}$
Sum of all respiratory flows	**1842.82**	1255.63	1263.5	411.31	2006	796.62	441.41	-	-	-	631.68	$t{\cdot}km^{-2}{\cdot}y^{-1}$
Sum of all flows into detritus	2465.63	1534.3	1194.21	**4565.27**	2630	1747.85	1127.4	-	-	-	1307.42	$t{\cdot}km^{-2}{\cdot}y^{-1}$
Total system throughput	8406.46	5883.14	4956.83	**10074.2**	9232	5914.87	3258.66	1831.93	1029.1	3096.5	4464.6	$t{\cdot}km^{-2}{\cdot}y^{-1}$
Sum of all production	3454.85	2660.61	2108.16	**4959.33**	3990.65	2455.23	1525.14	-	-	-	1921.36	$t{\cdot}km^{-2}{\cdot}y^{-1}$
Calculated total net primary production	2708.80	2185.79	1807.64	**4817.5**	3578.4	1825.12	-	-	-	-	1169.18	$t{\cdot}km^{-2}{\cdot}y^{-1}$
Total primary production/total respiration	1.47	1.74	1.43	11.713	1.7484	2.29	2.96	-	**1.35**	-	1.85	dimensionless
Net system production	865.98	930.16	544.15	4406.19	-	1028.5	1307.73	-	-	-	**537.51**	$t{\cdot}km^{-2}{\cdot}y^{-1}$
Total primary production/total biomass	40.95	26.56	41.27	**168.79**	67.737	24.34	24.82	-	4.62	-	7.81	dimensionless
Total biomass/total throughput	0.012	0.009	-	0.003	-	-	0.016	0.04	**0.05**	-	0.034	year[1]
Total biomass (excluding detritus)	101.98	53.38	**154.01**	28.542	52.82	75	52.68	74.73	47.04	51.66	149.71	$t{\cdot}km^{-2}{\cdot}y^{-1}$
Total catch	0.98	1.56	-	2.164	-	**3.06**	-	-	-	2.25	0.84	$t{\cdot}km^{-2}{\cdot}y^{-1}$
Mean trophic level of the catch	3.52	3.18	-	2.99	-	3.37	-	-	-	3.51	**3.57**	dimensionless
Gross efficiency (catch/net p.p.)	0.0004	0.001	0.00095	0.00045	-	**0.002**	-	-	-	-	0.001	dimensionless
Connectance Index	0.282	0.279	0.36	0.341	**0.518**	-	0.15	-	-	-	0.18	dimensionless
System Omnivory Index	0.231	0.215	0.21	**0.276**	-	0.27	0.23	0.199	0.2	-	0.25	dimensionless
Shannon diversity Index	**2.577**	1.869		1.131	-	-	-	-	-	1.19	-	dimensionless
Finn's Cycling Index	10.44	8.40	9.83	8.92	8.45	9.73	-	12.86	11.3	13.83	**17.3**	%
Finn's mean path length	3.103	2.692	-	2.091	-	3.19	-	-	-	-	**3.78**	dimensionless
Ascendency	8401	5486	-	-	**8677**	-	2156.9	2156.9	1024.4	2459	-	$t{\cdot}km^{-2}{\cdot}y^{-1}$
Ecopath pedigree	0.69	0.65	0.64	0.43	0.65	0.69	0.39	-	**0.70**	0.44	0.65	dimensionless
Number of functional groups	26	19	22	23	14	52	51	37	27	27	33	groups

Data sources: [1] this study; [2] Lin et al. (2013); [3] Rahman et al. (2019); [4] Wang et al. (2019);[5] Corrales et al. (2022); [6] Romero et al. (2024); [7]Raoux et al. (2017); [8] Pezy et al. (2020); [9] Adgé et al. (2024); [10]Couce Montero et al. (2025);

(CI = 0.199) but far less than for the Rudong OWF (CI = 0.518), indicating a more complex web-like trophic interactions among functional groups in Zhuanghe OWF, except for these latter systems. The FCI of Zhuanghe OWF area (10.44) ranked fifth highest among all OWF ecosystems, indicating a low level of nutrient cycling compared with other OWF ecosystems (Table 3).

4. Discussion

In this study, Ecopath models were constructed to comprehensively evaluate the ecosystem structure and function of the Zhuanghe OWF and a control area with no wind farm. This study differs from other Ecopath models of OWFs as data were collected from both the OWF and control areas to provide the input parameters for the models from the area of interest. Functional groups in the OWF system were first categorized into hard substrate (turbine monopiles) and soft substrate communities based on their affinity to different sediment types. The control area was used as a reference to quantitatively assess the ecological effects of OWF development. Beyond analyzing biomass, TL, and ecotrophic efficiency, the study compared ecosystem parameters related to energy flow, nutrient dynamics, and overall system functioning between the two regions. Our results show that sessile organisms on turbine monopiles accounted for approximately 50 % of the total biomass (excluding primary producers and detritus) in the OWF area, compared with their absence in the control area, underscoring the dominant role of benthic communities in the OWF. Additionally, the OWF ecosystem exhibited a more complex food web structure, greater system scale, and higher maturity than the control. These findings from the Ecopath models, based on empirical data from the OWF and control area, provide empirical evidence that OWF development can have a positive influence on the structural integrity and functional dynamics of local marine ecosystems.

4.1. Effects of offshore wind farm on ecosystem structure

The development of the Zhuanghe OWF has positively influenced demersal fishes and other functional groups, resulting in significant alterations to the ecosystem structure. Sessile organisms, such as the blue mussel *Mytilus edulis* and other suspension-feeding invertebrates colonized the monopiles in the OWF, constituted over 50 % of the total biomass in the OWF, excluding detritus and phytoplankton. The colonization of the bivalves and other low-trophic-level organisms has increased food availability for fish and benthic species through predation and deposition of organic matter such as feces and dead organisms (Wilhelmsson et al., 2006; Maar et al., 2009). In our study area, numerous aquaculture floating rafts are located near the turbine monopiles (Gao et al., 2024), and contain dense populations of suspension-feeding organisms such as the bivalves *M. edulis* and *C. gigas*, which serve as a significant source of recruitment of mussel, oyster and other sessile organisms to the OWF monopiles (Dumbauld et al., 2009). Additionally, the OWF is situated in an open-shelf area dominated by tidal hydrodynamics and characterized by a pronounced tidal regime, with maximum and mean tidal ranges of 5.36–6.38 m and 3.67–4.01 m, respectively. These strong tides enhance water exchange, thereby promoting the dispersal and settlement of larvae (Li et al., 2013; Ashley et al., 2014; Lin et al., 2019). Most fish functional groups exhibited significantly greater biomass in the OWF area, particularly demersal species, which is consistent with the findings from other studies and their suggestion that OWFs act as "fish aggregation devices" (Langhamer, 2012; Degraer et al., 2020; Knorrn et al., 2024). For instance, our model showed that benthic fish biomass nearly doubled in the OWF area compared to the control area.

In addition to providing a substrate for sessile organisms, the installation of wind turbines may generate local turbulence around the structures. This turbulence can cause the resuspension of seabed sediments, releasing nutrients into the water column (Ogilvie and Mitchell, 1998), thereby promoting phytoplankton growth by supplying essential biogenic elements for photosynthesis (Justić et al., 1995). On the other hand, resuspension helps increase detritus biomass, enhancing its availability to filter feeders such as zooplankton and bivalves (Justić et al., 1995; Broström, 2008), whose biomass significantly increased in Zhuanghe OWF area. Therefore, zooplanktivorous fish are more frequently observed within the OWF area, which likely contributes to the increased biomass of larger benthic and pelagic predators such as *S. schlegelii* and *S. niphonius*. Moreover, this increase could be linked to fishery restrictions in the OWF area, as relevant regulations often designate it as a no-take zone (Schupp et al., 2021), thereby enabling it to function as a marine protected area (MPA) that offers refuge to commercially targeted species (Coates et al., 2016).

The comparison of TLs of all functional groups in the OWF and control ecosystem indicated that TLs in the OWF were generally higher across all groups except for zooplankton, phytoplankton, and detritus, which showed no significant changes. These results suggest potential alterations in species composition within functional groups and shifts in the trophic relationships of the OWF area. Possibly due to reef effect, new species were attracted which increase predation pressure, thereby providing an additional prey resource for higher trophic levels. However, comparison of EEs for benthic fish groups *H. otakii,* and *S. schlegelii* between the OWF and control site showed minor differences. EEs indicate the fraction of production utilized within the system, via trophic transfer, biomass accumulation, migration, or export. Slightly elevated EEs for these rocky-reef fishes at the OWF likely reflect reef-associated habitat effects and higher fishing pressure relative to the control area.

The MTI analyses, showed that *H. otakii* was negatively impacted by *S. schlegelii*, likely due to their overlapping ecological niches and feeding habits, leading to resource competition (Wu et al., 2019; Zhang et al., 2021). *Charybdis japonica*, other crustaceans and demersal forage fish are the common prey species for both *H. otakii* and *S. schlegelii*. Our models also showed that other soft substrate crustaceans and zooplanktivorous fish are key groups in energy and nutrient transfer from planktonic primary and secondary producers to higher-level predators. Middle TL organisms were found to exert top-down control on zooplankton and benthos, while higher-order predators were subject to bottom-up control. Such mechanisms have typically been observed in small plankton-feeding pelagic species, like anchovies and sardines (Bakun, 2006; Coll et al., 2006). However, in the OWF area, this role of pelagic plankton-feeders appears to have been replaced by soft-substrate crustaceans. This shift reflects the transition from a benthopelagic to a more benthic-dominated system in the OWF (Nogues et al., 2021). *Sebastes schlegelii* exhibited the highest keystone index and relative

total impact index in both the OWF and control area, underscoring its role in top-down food web regulation and contributing to ecosystem health and stability. This finding suggests that the importance of the “fish-benthos” community is not only attributed to the aggregation effects linked to the "reef effect" (Reubens et al., 2013) but also to its specific position in the food web, which ultimately determines its high keystone index. Additionally, the reduced commercial fishing pressure in the OWF area functioned similarly to a fishing exclusion zone, likely to further enhance the ecological significance of the OWF area.

4.2. *Effects of the offshore wind farm on ecosystem function*

The overall transfer efficiencies in the Ecopath model for the OWF and control area were slightly higher than those reported by Lindeman (1942) (10 %) and (Pauly and Christensen, 1995) (10.1 % across 48 aquatic communities), but lower than the 15 % reported by Ryther (1969). Notably, energy transfer efficiency was greater in the OWF area than the control area, particularly from TLs II to III. This suggests that lower trophic levels play a crucial role in energy transfer. In the OWF area, the detritus transfer efficiency exceeded that of phytoplankton, likely due to benthic organisms’ higher consumption of detritus. This finding could indicate a shift in the food web from primary producers and grazers towards a detritus-feeding community, as evidenced by the high energy efficiency of detritus (Norling and Kautsky, 2007; Maar et al., 2009). A similar pattern was observed in the Rudong OWF in Jiangsu Province, China, where an increase in energy flow through the detrital food chain was reported, although the system remained dominated by grazers (Wang et al., 2019). Likewise, in the Courseulles-sur-Mer OWF, detritivory within the food web intensified in areas containing monopile structures, underscoring the important role of trophic interactions in the detrital pathway (Raoux et al., 2017).

The hard substrate of the artificial structures in the OWF added habitat heterogeneity to the otherwise sandy area, and appears to enhance energy flow diversity, which is associated with higher species diversity (Christensen, 1995; Munguia et al., 2011). Organic materials released by higher TL organisms like fish and crustaceans near the turbine monopiles increase the abundance of zoobenthic feeders and their predators (Maar et al., 2009; Raoux et al., 2017). This direct flow of organic material from turbine monopiles to benthic communities creates shortcuts in the food chain, linking high- and low-trophic species (Raoux et al., 2017). Primary producers also benefit from the resource sharing facilitated by OWFs. For instance, phytoplankton growth rates are improved by additional food for mussels or by increased ammonium excretion from suspension-feeders, reducing turbidity (Norling and Kautsky, 2007). In summary, the redistribution of resources has led marine food webs to evolve towards a more sustainable, harmonious, and complex state, reducing trophic competition in OWF areas. This evolution has enhanced the system’s ability to withstand disturbances (Levin and Lubchenco, 2008), improving its resilience and resistance to stress. These transformations are linked to increased benthic biomass, positively affecting ecosystem complexity, efficiency, diversity, and resilience (Nogues et al., 2021).

According to the scenarios simulated by Raoux et al. (2017) and Wang et al. (2019), the construction of OWFs is expected to lead to increases in total system throughput, ecosystem activity, recycling, and the magnitude of detritivorous flows. These expectations are consistent with the findings from our study based on ecosystem models with empirical data for areas with and without OWF. For example, the significant increases in FCI and MPL observed in the OWF area indicate an improved capacity for energy recycling, while the elevated ascendency reflects higher overall ecosystem activity. In addition, the slightly higher values of the CI and SOI in the OWF area suggest a gradual strengthening of internal ecosystem stability. Although the SOI values for both the OWF and control areas indicate a predominantly chain-like food web structure (Table 3), the marginally higher SOI observed in the OWF area is noteworthy, as a higher SOI generally signifies a more resilient and flexible ecosystem (Fagan, 1997; Libralato, 2008). Furthermore, the Shannon diversity index was higher in the OWF area compared to the control, suggesting that the OWF area has a greater diversity and biomass is more evenly distributed among many functional groups. When compared with other OWFs worldwide that have undergone longer post-construction periods, the Zhuanghe OWF, with only two years since its construction, remains at a developing stage of ecosystem maturity. This is evident in comparisons with both field-based simulation studies, such as the Rudong OWF in China (5 years after construction, Wang et al., 2019), and long-term dynamic modelling approaches, including the Gruissan Coast OWF in France (30 years after construction, Adgé et al., 2024) and the Fuerteventura and Lanzarote islands OWF in Spain (28 years after construction, Couce Montero et al., 2025).

4.3. *Limitations and future development of this study*

By employing an ecosystem modelling framework, this study enabled a more holistic understanding of the far-reaching effects of OWF development on the coastal waters of northern China. In our current study, functional groups were specifically and clearly categorized by habitat type, encompassing soft-substrate communities present at both sites and hard-substrate communities associated with turbine monopiles. A key strength of our study lies in incorporating the components of sessile organisms attached to the hard surface of monopiles in the OWF and their associated reef fish, highlighting their trophic function by setting up the respective functional groups and identifying their trophic links in the OWF area. Adge et al. (2024) provided evidence for the vital ecological role of sessile organisms in enhancing the total system throughput and ecosystem maturity by simulating the increase of specific target sessile organisms to represent the reef effect in the Gulf of Lion in the Mediterranean Sea. The results could be considered as a novel perspective in assessing offshore wind farm impacts on marine ecosystems through food web modelling. The study documents fundamental shifts in both the structure and function of the OWF ecosystem compared with the control area. Overall, these findings provide valuable insights into how OWFs affect coastal ecosystems and offer scientific support for evaluating their ecological impacts and guiding future OWF planning.

The present study focused primarily on a short period of the OWF’s operational phase. However, previous research suggests that the succession of sessile organisms on OWF structures takes more than 6 years to reach a stable climax community, emphasizing the

importance of long-term monitoring and assessment to fully understand coastal ecosystem responses to OWF developments (Kerckhof et al., 2019). Moreover, OWF ecosystems may be subject to cumulative pressures from climate change and nearby aquaculture activities. Future studies should integrate long-term data across broader spatial scales to simulate and evaluate the cumulative impacts of OWFs on coastal ecosystems.

Spillover effects are well-documented phenomenon around no-take marine reserves, but they generally occur over relatively small spatial scales (Di Lorenzo et al., 2020; Amelot et al., 2024). Similarly, OWF have exhibited localized spillover effects, with increased biomass and catches concentrated in areas immediately adjacent to turbine structures. Halouani et al. (2020) showed that, for most functional groups, spillover is typically confined to within ~3 km around the OWF and declines sharply with distance, particularly for commercial and demersal species. In the present study, although the two modelled areas are separated by more than 6 km, the movement of plankton and nekton introduces some uncertainty in model comparisons, as the population dynamics and home ranges of mobile species often extend beyond the site boundaries. Nevertheless, the dominant biomass in both models is primarily composed of sessile organisms, reef-associated fishes, and invertebrates with limited mobility, which largely shape the trophic structure of the ecosystem. For example, the two dominant rocky reef fishes, *H. otakii* and *S. schlegelii*, are resident species that inhabit the area year-round, exhibiting strong habitat fidelity and restricted movement (Kanamoto, 1979; Zhang et al., 2015). Future studies should investigate habitat utilization to better understand the responses of pelagic and migratory fishes to OWF development, and applying the Ecospace model could help project the spatial dynamics of these mobile organisms.

5. Conclusions

Two Ecopath models, based on comprehensive field survey data, were developed to represent the coastal ecosystems of the northern Yellow Sea, i.e. with and without OWF installation. By comparing ecosystem structure and function between the OWF site and an adjacent control area, this study assessed the ecological impacts of OWF development on coastal marine systems. Overall, the establishment of the OWF exerted positive effects on both the structural and functional components of the ecosystem. The introduction of turbine monopiles provided new habitats for sessile organisms, leading to a shift in community composition toward benthic dominance. This habitat modification resulted in greater biomass and production of benthic fishes in the OWF area compared to the control, indicating a potential reef effect associated with the turbine foundations. The OWF ecosystem exhibited a more complex trophic structure and higher total energy transfer efficiency than in the control area, with trophic flows shifting from primary producer–dominated to detritus-driven pathways. Despite the relatively recent construction of the Zhuanghe OWF, the ecosystem is showing signs of progressing toward greater ecological maturity, with higher overall activity, diversity, stability, and functional integrity. Furthermore, the aggregation of high-trophic-level, reef-associated fish species around the turbine foundations, which are exclusively targeted by recreational anglers, has increased the mean trophic level of catches in the OWF-occupied coastal ecosystem, indicating a no-take marine reserve effect within the OWF area. Collectively, these findings provide a foundation for understanding how OWF development influences ecosystem energy dynamics and fishery resources in coastal waters. They highlight the potential of OWFs to enhance local biodiversity and ecological functioning, while also informing sustainable management strategies for marine renewable energy development.

CRediT authorship contribution statement

Zhongxin Wu: Writing – review & editing, Writing – original draft, Supervision, Methodology, Investigation, Funding acquisition, Conceptualization. **Tao Tian:** Resources, Conceptualization. **Longfei Xu:** Methodology, Investigation, Formal analysis. **Liwei Si:** Writing – review & editing, Writing – original draft, Visualization, Resources, Investigation, Formal analysis, Data curation. **Tweedley James:** Writing – review & editing, Visualization, Methodology. **Zhilin Wang:** Methodology, Investigation, Formal analysis. **Yi Li:** Investigation. **Loneragan Neil:** Writing – review & editing, Visualization, Methodology. **Hang Liu:** Investigation.

Declaration of Competing Interest

The authors declare that they have no known competing financial interests or personal relationships that could have appeared to influence the work reported in this paper.

The authors declare the following financial interests/personal relationships which may be considered as potential competing interests.

Acknowledgements

Gratitude is expressed to members from the Center for Marine Ranching Engineering Science Research of Liaoning Province at Dalian Ocean University, particularly to Xu Wei, Wencong An, Yanchao Zhang for their assistance during the period of sampling in this study. The authors also thank the following funding providers for supporting the research: General Program of Liaoning Provincial Joint Foundation (2023-MSLH-018), National Key Research & Development Program of China (2024YFD2401803, 2023YFD2401102), General Program of Liaoning Provincial Department of Education (LJKMZ20221120). We thank the reviewers and editors for their constructive comments on our manuscript.

Appendix A. Supporting information

Supplementary data associated with this article can be found in the online version at doi:10.1016/j.gecco.2025.e03982.

Data availability

Data will be made available on request.

References

Abramic, A., Cordero-Penin, V., Haroun, R., 2022. Environmental impact assessment framework for offshore wind energy developments based on the marine Good Environmental Status. Environ. Impact Assess. Rev. 97, 106862. https://doi.org/10.1016/j.eiar.2022. 106862.

Adgé, M., Lobry, J., Tessier, A., Planes, S., 2024. Modeling the impact of floating offshore wind turbines on marine food webs in the Gulf of Lion, France. Front. Mar. Sci. 11, 1379331. https://doi.org/10.3389/fmars.2024.1379331.

Amelot, M., Normand, J., Schlaich, I., Ernande, B., 2024. Spillover and competitive exclusion in the crustacean community following the implementation of a marine reserve. ICES J. Mar. Sci. 81 (9), 1827–1836. https://doi.org/10.1093/icesjms/fsae128.

Ashley, M.C., Mangi, S.C., Rodwell, L.D., 2014. The potential of offshore windfarms to act as marine protected areas–a systematic review of current evidence. Mar. Pol. 45, 301–309. https://doi.org/10.1016/j.marpol.2013.09.002.

Bailey, H., Brookes, K.L., Thompson, P.M., 2014. Assessing environmental impacts of offshore wind farms: lessons learned and recommendations for the future. Aquat. Biosyst. 10, 8. https://doi.org/10.1186/2046-9063-10-8.

Bakun, A., 2006. Wasp-waist populations and marine ecosystem dynamics: navigating the "predator pit" topographies. Prog. Oceano 68, 271–288. https://doi.org/10.1016/j.pocean, 2006.02.004.

Bicknell, A.W., Gierhart, S., Witt, M.J., 2025. Site and species dependent effects of offshore wind farms on fish populations. Mar. Environ. Res. 106977. https://doi.org/10.1016/j marenvres.2025.106977.

Broström, G., 2008. On the influence of large wind farms on the upper ocean circulation. J. Mar. Syst. 74 (1-2), 585–591. https://doi.org/10.1016/j.jmarsys.2008.05.001.

Cheng, J., 2004. Marine ecological environment and biological communities in the coastal waters of the Yellow Sea and Bohai Sea. China Ocean University Press.

Christensen, V., 1995. Ecosystem maturity—towards quantification. Ecol. Model 77, 3–32. https://doi.org/10.1016/0304-3800(93)E0073-C.

Christensen, V., Pauly, D., 1992. ECOPATH II—a software for balancing steady-state ecosystem models and calculating network characteristics. Ecol. Model 61, 169–185. https://doi.org/10.1016/0304-3800(92)90016-8.

Christensen, V., Walters, C.J., 2004. Ecopath with Ecosim: methods, capabilities and limitations. Ecol. Model 172, 109–139. https://doi.org/10.1016/j.ecolmodel.2003.09.003.

Christensen, V., Walters, C., Pauly, D., 2005. Ecopath with Ecosim: A User's Guide. Fisheries Centre, University of British Columbia, Vancouver, Canada and ICLARM, Penang, Malaysia.

Coates, D.A., Kapasakali, D.A., Vincx, M., Vanaverbeke, J., 2016. Short-term effects of fishery exclusion in offshore wind farms on macrofaunal communities in the Belgian part of the North Sea. Fish. Res. 179, 131–138. https://doi.org/10.1016/j.fishres.2016.02.019.

Coll, M., Palomera, I., Tudela, S., Sardà, F., 2006. Trophic flows, ecosystem structure, and fishing impacts in the South Catalan Sea, Northwestern Mediterranean. J. Mar. Syst. 59, 63–96. https://doi.org/10.1016/j.jmarsys.2005.09.001.

Coolen, J.W., Bittner, O., Driessen, F.M., van Dongen, U., Siahaya, M.S., de Groot, W., Mavraki, N., Bolam, S.G., van der Weide, B., 2020. Ecological implications of removing a concrete gas platform in the North Sea. J. Sea Res. 166, 101968. https://doi.org/10.1016/j.seares.2020.101968.

Corrales, X., Preciado, I., Gascuel, D., de Gamiz-Zearra, A.L., Hernvann, P.Y., Mugerza, E., Andonegi, E., 2022. Structure and functioning of the Bay of Biscay ecosystem: a trophic modelling approach. Estuar. Coast. shelf Sci. 264, 107658. https://doi.org/10.1016/j.ecss.2021.107658.

Couce Montero, L., Abramic, A., Guerra Marrero, A., Espino Ruano, A., Jiménez Alvarado, D., Castro Hernández, J.J., 2025. Addressing offshore wind farms compatibilities and conflicts with marine conservation through the application of modelled benchmarking scenarios. Renew. Sustain. Energy Rev. 207, 114894. https://doi.org/10.1016/j.rser.2024.114894.

Cui, P.D., Bian, X.D., Zhang, Y.X., Shan, X.J., Jin, X.S., Zhao, Y.S., Wang, H.B., 2024. Community structure of fishery organisms in offshore waters of the North Yellow Sea, 049314-1 J. Fish. China 48 (4). https://doi.org/10.11964/jfc.20220713605.

Degraer, S., Carey, D.A., Coolen, J.W., Hutchison, Z.L., Kerckhof, F., Rumes, B., Vanaverbeke, J., 2020. Offshore wind farm artificial reefs affect ecosystem structure and functioning. Oceanography 33, 48–57. https://doi.org/10.5670/oceanog.2020.405.

Di Lorenzo, M., Guidetti, P., Di Franco, A., Calò, A., Claudet, J., 2020. Assessing spillover from marine protected areas and its drivers: a meta-analytical approach. Fish Fish. 21 (5), 906–915. https://doi.org/10.1111/faf.12469.

Dumbauld, B.R., Ruesink, J.L., Rumrill, S.S., 2009. The ecological role of bivalve shellfish aquaculture in the estuarine environment: a review with application to oyster and clam culture in West Coast (USA) estuaries. Aquac 290 (3-4), 196–223. https://doi.org/10.1016/j.aquaculture.2009.02.033.

Fagan, W.F., 1997. Omnivory as a stabilizing feature of natural communities. Am. Nat. 150, 554–567. https://doi.org/10.1086/286081.

Finn, J.T., 1976. Measures of ecosystem structure and function derived from analysis of flows. J. Theor. Biol. 56, 363–380. https://doi.org/10.1016/S0022-5193(76)80080-X.

Gao, L., Kong, N., Liu, R.Y., Zhao, J.Y., Xing, Z., Zhang, Z.Y., Song, L.S., 2024. Investigation on the variation of environmental factors, glycogen and immune parameters of Pacific oyster (*Crassostrea gigas*) in the North Yellow Sea shellfish farming area in summer, 049413-1 J. Fish. China 48 (4). https://doi.org/10.11964/jfc.20220313357.

Garthe, S., Schwemmer, H., Peschko, V., Markones, N., Müller, S., Schwemmer, P., Mercker, M., 2023. Large-scale effects of offshore wind farms on seabirds of high conservation concern. Sci. Rep. 13 (1), 4779. https://doi.org/10.1038/s41598-023-31601-z.

Gill, A.B., Degraer, S., Lipsky, A., Mavraki, N., Methratta, E., Brabant, R., 2020. Setting the context for offshore wind development effects on fish and fisheries. Oceanography 33, 118–127. https://doi.org/10.5670/oceanog.2020.411.

Global Wind Energy Council (GWEC), 2024. Global Offshore Wind Report 2024. Brussels, Belgium.

Gușatu, L.F., Menegon, S., Depellegrin, D., Zuidema, C., Faaij, A., Yamu, C., 2021. Spatial and temporal analysis of cumulative environmental effects of offshore wind farms in the North Sea basin. Sci. Rep. 11, 10125. https://doi.org/10.1038/s41598-021-89537-1.

Halouani, G., Villanueva, C.M., Raoux, A., Dauvin, J.C., Lasram, F.B.R., Foucher, E., Niquil, N., 2020. A spatial food web model to investigate potential spillover effects of a fishery closure in an offshore wind farm. J. Mar. Syst. 212, 103434. https://doi.org/10.1016/j.jmarsys.2020.103434.

Justić, D., Rabalais, N.N., & Turner, R.E. (1995. Stoichiometric nutrient balance and origin of coastal eutrophication. Mar. pollut. bull. 30(1), 41-46. https://doi.org/10.1016/0025-326X(94)00105-I.

Kerckhof, F., Rumes, B., Degraer, S., 2019. About "Mytilisation" and "Slimeification": a decade of succession of the fouling assemblages on wind turbines off the Belgian coast, in: Degraer, S. et al. Environmental impacts of offshore wind farms in the Belgian part of the North Sea: making a decade of monitoring, research and innovation. Memoirs on the Marine Environment, pp. 73–84 In: Degraer, S. et al. 2019. Environmental impacts of offshore wind farms in the Belgian part of

the North Sea: making a decade of monitoring, research and innovation. Memoirs on the Marine Environment. Royal Belgian Institute of Natural Sciences, OD Natural Environment, Marine Ecology and Management Section: Brussels. ISBN 978–9–0732-4249-4.
Kanamoto, A., 1979. On the ecology of Hexagrammid fish 5. Food items of *Agrammus agrammus* and *Hexagrammos otakii* sampled from different habitats around a small reef. Jap. J. Ecol. 29, 265–271. https://doi.org/10.18960/seitai.29.2_171.
Knorrn, A.H., Teder, T., Kaasik, A., Kreitsberg, R., 2024. Beneath the blades: marine wind farms support parts of local biodiversity - a systematic review. Sci. Total Environ. 935, 173241. https://doi.org/10.1016/j.scitotenv.2024.173241.
Langhamer, O., 2012. Artificial reef effect in relation to offshore renewable energy conversion: state of the art. Sci. World J., 386713 https://doi.org/10.1100/2012/386713.
Lemasson, A.J., Somerfield, P.J., Schratzberger, M., Thompson, M.S., Firth, L.B., Couce, E., Knights, A.M., 2024. A global meta-analysis of ecological effects from offshore marine artificial structures. Nat. Sustain 7 (4), 485–495. https://doi.org/10.1038/s41893-024-01311-z.
Leonhard, S.B., Pedersen, J., 2005. Hard bottom substrate monitoring Horns Rev offshore wind farm. Annual status report. https://www.osti.gov/etdeweb/biblio/20780426.
Leonhard, S.B., Stenberg, C., Støttrup, J.G., 2011. Effect of the Horns Rev 1 offshore wind farm on fish communities: follow-up seven years after construction. Danish Energy Authority. https://doi.org/10.20935/AcadQuant7594.
Levin, S.A., Lubchenco, J., 2008. Resilience, robustness, and marine ecosystem-based management. Bioscience 58, 27–32. https://doi.org/10.1641/B580107.
Li, X., Xie, M.X., Li, M.G., 2013. Numerical modeling of the hydrodynamics for Zhuanghe fishing port. Adv. Mat. Res. 765, 2952–2956. https://doi.org/10.4028/www.scientific.net/AMR, 765-767.2952.
Li, X.W., Zhao, J.M., Liu, H., Zhang, H., Hou, X.Y., 2018. Status, problems and optimized management of spawning, feeding, overwintering grounds and migration route of marine fishery resources in Bohai Sea and Yellow Sea. Chin. J. Oceanol. Limnol. 5, 147–157. https://doi.org/10.13984/j.cnki.cn37-1141.2018.05.019.
Libralato, S., 2008. System Omnivory Index. Encyclopedia of Ecology (Second Edition). https://doi.org/10.1016/B978-0-12-409548-9.00605-9.
Libralato, S., Christensen, V., Pauly, D., 2006. A method for identifying keystone species in food web models. Ecol. Model 195, 153–171. https://doi.org/10.1016/j.ecolmodel, 2005.11.029.
Lin, F., Asplin, L., Budgell, W.P., Wei, H., Fang, J., 2019. Currents on the northern shelf of the Yellow Sea. Reg. Stud. Mar. Sci. 32, 100821. https://doi.org/10.1016/j.rsma. . 2019.100821.
Lin, Q., Jin, X., Zhang, B., 2013. Trophic interactions, ecosystem structure and function in the southern Yellow Sea. Chin. J. Oceanol. Limnol. 31, 46–58. https://doi.org/10.1007/s00343, 013-2013-6.
Lindeboom, H.J., Kouwenhoven, H.J., Bergman, M.J.N., Bouma, S., Brasseur, S., Daan, R., Fijn, R.C., De Haan, D., Dirksen, S., Van Hal, R., 2011. Short-term ecological effects of an offshore wind farm in the Dutch coastal zone; a compilation. Environ. Res. Lett. 6, 035101. https://doi.org/10.1088/1748-9326/6/3/035101.
Lindeman, R.L., 1942. The trophic-dynamic aspect of ecology. Ecology 23, 399–417. https://doi.org/10.2307/1930126.
Link, J.S., 2010. Adding rigor to ecological network models by evaluating a set of pre-balance diagnostics: a plea for PREBAL. Ecol. Model 221, 1580–1591. https://doi.org/10.1016/j.ecolmodel.2010.03.012.
Liu, C.Y., Jiang, S.Y., Song, B., 2020. Food web structure of macrobenthos in the intertidal zone of Yangma Island. Yantai. China 51, 467–476. https://doi.org/10.11693/hyhz20191100217.
Liu, H.Y., Yang, C.J., Zhang, P.D., Li, W.T., Zhang, X.M., 2019. An Ecopath evaluation of system structure and function for the Laoshan Bay artificial reef zone ecosystem. Acta Ecol. Sin. 39, 3926–3936. https://doi.org/10.5846/stxb201805301193.
Lovich, J.E., Ennen, J.R., 2013. Assessing the state of knowledge of utility-scale wind energy development and operation on non-volant terrestrial and marine wildlife. Appl. Energy 103, 52–60. https://doi.org/10.1016/j.apenergy.2012.10.001.
Lozano-Montes, H., Loneragan, N.R., Fourie, S.A., Fulton, E.A., Yeoh, D., 2025. Ecological network analysis and ecological indicators for an intensively used temperate marine embayment. Estuar. Coast. Shelf Sci. 320, 109285. https://doi.org/10.1016/j.ecss.2025.109285.
Maar, M., Bolding, K., Petersen, J.K., Hansen, J.L., Timmermann, K., 2009. Local effects of blue mussels around turbine foundations in an ecosystem model of Nysted off-shore wind farm, Denmark. J. Sea Res. 62, 159–174. https://doi.org/10.1016/j.seares.2009.01.008.
Ministry of Agriculture and Rural Affairs, 2023. Bureau of Fisheries (MARA-BF). China Fishery Statistical Yearbook. China Agriculture Press, Beijing.
Ministry of Agriculture and Rural Affairs, 2024. Bureau of Fisheries (MARA-BF). China Fishery Statistical Yearbook. China Agriculture Press, Beijing.
Mueller-Blenkle, C., McGregor, P.K., Gill, A.B., Andersson, M.H., Metcalfe, J., Bendall, V., Sigray, P., Wood, D.T., Thomsen, F., 2010. Effects of pile-driving noise on the behaviour of marine fish. http://dspace.lib.cranfield.ac.uk/handle/1826/8235.
Munguia, P., Osman, R.W., Hamilton, J., Whitlatch, R., Zajac, R., 2011. Changes in habitat heterogeneity alter marine sessile benthic communities. Ecol. Appl. 21, 925–935. https://doi.org/10.1890/09-2398.1.
Ning, X.R., Liu, Z.L., Shi, J.X., 1995. Evaluation of primary productivity and potential fishery production of Bohai Sea: Yellow sea and East China Sea. Acta Oceanol. Sin. 17, 72–84. https://doi.org/10.1088/0256-307X/12/7/010.
Nogues, Q., Raoux, A., Araignous, E., Chaalali, A., Hattab, T., Leroy, B., Ben Rais Lasram, F., David, V., Le Loc'h, F., Dauvin, J.-C., Niquil, N., 2021. Cumulative effects of marine renewable energy and climate change on ecosystem properties: sensitivity of ecological network analysis. Ecol. Indic. 121, 107128. https://doi.org/10.1016/j.ecolind.2020.107128.
Norling, P., Kautsky, N., 2007. Structural and functional effects of *Mytilus edulis* on diversity of associated species and ecosystem functioning. Mar. Ecol. Prog. Ser. 351, 163–175. https://doi.org/10.3354/meps07033.
Odum, E.P., 1969. The strategy of ecosystem development. Science. https://doi.org/10.1126/science.164.3877.262.
Ogilvie, B.G., Mitchell, S.F., 1998. Does sediment resuspension have persistent effects on phytoplankton? Experimental studies in three shallow lakes. Freshw. Biol. 40 (1), 51–63. https://doi.org/10.1046/j.1365-2427.1998.00331.x.
Palomares, M.L.D., Pauly, D., 1998. Predicting food consumption of fish populations as functions of mortality, food type, morphometrics, temperature and salinity. Mar. Freshw. Res 49, 447–453. https://doi.org/10.1071/MF98015.
Pauly, D., 1980. On the interrelationships between natural mortality, growth parameters, and mean environmental temperature in 175 fish stocks. ICES J. Mar. Sci. 39, 175–192. https://doi.org/10.1093/icesjms/39.2.175.
Pauly, D., Christensen, V., 1995. Primary production required to sustain global fisheries. Nature 374 (6519), 255–257. https://doi.org/10.1038/374255a0.
Pauly, D., Soriano-Bartz, M.L., Palomares, M.L.D., 1993. Improved construction, parametrization and interpretation of steady-state ecosystem models, in: trophic Models of Aquatic Ecosystems. ICLARM Conf. Proc. 1–13.
Petersen, J.K., Malm, T., 2006. Offshore windmill farms: threats to or possibilities for the marine environment. AMBIO A J. Hum. Environ. 35, 75–80. https://doi.org/10.1579/0044-7447(2006)35[75:OWFTTO]2.0.CO;2.
Pezy, J.-P., Raoux, A., Dauvin, J.-C., 2020. The environmental impact from an offshore windfarm: Challenge and evaluation methodology based on an ecosystem approach. Ecol. Indic. 114, 106302. https://doi.org/10.1016/j.ecolind.2020.106302.
Polovina, J.J., 1984. Model of a coral reef ecosystem. Coral Reefs 3, 1–11. https://doi.org/10.1007/BF00306135.
Premalatha, M., Abbasi, T., Abbasi, S.A., 2014. Wind energy: increasing deployment, rising environmental concerns. Renew. Sustain. Energy Rev. 31, 270–288. https://doi.org/10.1016/j.rser.2013.11.019.
Rahman, M.F., Qun, L., Xiujuan, S., Chen, Y., Ding, X., Liu, Q., 2019. Temporal changes of structure and functioning of the Bohai Sea ecosystem: Insights from Ecopath models. Thalass. Int. J. Mar. Sci. 35, 625–641. https://doi.org/10.1007/s41208-019-00139-1.
Raoux, A., Tecchio, S., Pezy, J.-P., Lassalle, G., Degraer, S., Wilhelmsson, D., Cachera, M., Ernande, B., Le Guen, C., Haraldsson, M., Grangeré, K., Le Loc'h, F., Dauvin, J.-C., Niquil, N., 2017. Benthic and fish aggregation inside an offshore wind farm: which effects on the trophic web functioning? Ecol. Indic. 72, 33–46. https://doi.org/10.1016/j.ecolind.2016.07.037.
Raoux, A., Lassalle, G., Pezy, J.-P., Tecchio, S., Safi, G., Ernande, B., Mazé, C., Loc'h, F.L., Lequesne, J., Girardin, V., Dauvin, J.-C., Niquil, N., 2019. Measuring sensitivity of two OSPAR indicators for a coastal food web model under offshore wind farm construction. Ecol. Indic. 96, 728–738. https://doi.org/10.1016/j.ecolind.2018.07.014.

Reubens, J.T., Braeckman, U., Vanaverbeke, J., Van Colen, C., Degraer, S., Vincx, M., 2013. Aggregation at windmill artificial reefs: CPUE of Atlantic cod (*Gadus morhua*) and pouting (*Trisopterus luscus*) at different habitats in the Belgian part of the North Sea. Fish. Res. 139, 28–34. https://doi.org/10.1016/j.fishres.2012.10.011.

Romero, J., Alonso, H., Freitas, L., Granadeiro, J.P., 2024. Food web of the oceanic region of the archipelago of Madeira: the role of marine megafauna in the subtropical northeast Atlantic ecosystem. Mar. Environ. Res. 195, 106382. https://doi.org/10.1016/j.marenvres.2024.106382.

Rumes, B., Coates, D., De Mesel, I., Derweduwen, J., Kerckhof, F., Reubens, J., Vandendriessche, S., 2013. Changes in species richness and biomass at different spatial scales. In: Degraer, S., Brabant, R., Rumes, B. (Eds.), Environmental Impacts of Offshore Wind Farms in the Belgian Part of the North Sea: Learning From the Past to Optimise Future Monitoring Programmes.Royal Belgian Institute of Natural Sciences, Operational Directorate Natural Environment. Marine Ecology and Management, Brussels, pp. 183–189. https://doi.org/10.1086/285019.

Ryther, J.H., 1969. Photosynthesis and Fish Production in the Sea: The production of organic matter and its conversion to higher forms of life vary throughout the world ocean. Science 166 (3901), 72–76. https://doi.org/10.1126/science.166.3901.72.

Schupp, M.F., Kafas, A., Buck, B.H., Krause, G., Onyango, V., Stelzenmüller, V., Davies, I., Scott, B.E., 2021. Fishing within offshore wind farms in the North Sea: stakeholder perspectives for multi-use from Scotland and Germany. J. Environ. Manag 279, 111762. https://doi.org/10.1016/j.jenvman.2020.111762.

Shields, M.A., Payne, A.I., 2014. Marine renewable energy technology and environmental interactions. Springer, London, New York.

Stock, A., Murray, C.C., Gregr, E.J., Steenbeek, J., Woodburn, E., Micheli, F., Christensen, V., Chan, K.M.A., 2023. Exploring multiple stressor effects with Ecopath, Ecosim, and Ecospace: Research designs, modeling techniques, and future directions. Sci. Total Environ. 869, 161719. https://doi.org/10.1016/j.scitotenv.2023.161719.

Teilmann, J., Carstensen, J., 2012. Negative long term effects on harbour porpoises from a large scale offshore wind farm in the Baltic—evidence of slow recovery. Environ. Res. Lett. 7, 045101. https://doi.org/10.1088/1748-9326/7/4/045101.

Ulanowicz, R.E., Puccia, C.J., 1990. Mixed trophic impacts in ecosystems. Coenoses. 7–16. https://www.jstor.org/stable/43461017.

Wang, J., Zou, X., Yu, W., Zhang, D., Wang, T., 2019. Effects of established offshore wind farms on energy flow of coastal ecosystems: a case study of the Rudong offshore wind farms in China. Ocean Coast. Manag 171, 111–118. https://doi.org/10.1016/j.ocecoaman.2019.01.016.

Wang, R., Li, C., Wang, K.E., Zhang, W., 1998. Feeding activities of zooplankton in the Bohai Sea. Fish. Oceano 7, 265–271. https://doi.org/10.1046/j.1365-2419.1998.00067.x.

Watson, S.C., Somerfield, P.J., Lemasson, A.J., Knights, A.M., Edwards-Jones, A., Nunes, J., Beaumont, N.J., 2024. The global impact of offshore wind farms on ecosystem services. Ocean Coast. Manag. 249, 107023.

Wilhelmsson, D., Malm, T., 2008. Fouling assemblages on offshore wind power plants and adjacent substrata. Estuar. Coast. Shelf Sci. 79, 459–466. https://doi.org/10.1016/j.ecss.2008.04.020.

Wilhelmsson, D., Malm, T., Öhman, M.C., 2006. The influence of offshore windpower on demersal fish. ICES J. Mar. Sci. 63 (5), 775–784. https://doi.org/10.1016/j.icesjms.2006. 02.001.

Wu, Z., Zhang, X., Dromard, C.R., Tweedley, J.R., Loneragan, N.R., 2019. Partitioning of food resources among three sympatric scorpionfish (Scorpaeniformes) in coastal waters of the northern Yellow Sea. Hydrobiologia 826, 331–351. https://doi.org/10.1007/s10750-018-3747-0.

Wu, Z.X., Zhang, X.M., Lozano-Montes, H.M., Loneragan, N.R., 2016. Trophic flows, kelp culture and fisheries in the marine ecosystem of an artificial reef zone in the Yellow Sea. Estuar. Coast. Shelf Sci. 182, 86–97. https://doi.org/10.1016/j.ecss.2016.08.021.

Yang, H.S., Ru, X.S., Zhang, L.B., Lin, C.G., 2019. Industrial convergence of marine ranching and offshore wind power: Concept and prospect. Bull. Chin. Acad. Sci. 34, 700–707. https://doi.org/10.16418/j.issn.1000-3045.2019.06.011.

Yang, J.M., 2001. A study on food and trophic levels of Bohai Sea invertebrates. Mod. Fish. Inf. 16, 8–16. https://doi.org/10.3969/j.issn.1004-8340.2001.09.002.

Zettler, M.L., Pollehne, F., 2006. The impact of wind engine constructions on benthic growth patterns in the Western Baltic. In: Köller, J., Köppel, J., Peters, W. (Eds.), Offshore Wind Energy: Research on Environmental Impacts. Springer, Berlin, Heidelberg, New York, pp. 201–222.

Zhang, R., Liu, H., Zhang, Q., Zhang, H., Zhao, J., 2021. Trophic interactions of reef-associated predatory fishes (*Hexagrammos otakii* and *Sebastes schlegelii*) in natural and artificial reefs along the coast of North Yellow Sea, China. Sci. Total Enviro 791, 148250. https://doi.org/10.1016/j.scitotenv.2021.148250.

Zhang, Y., Xu, Q., Alos, J., Liu, H., Xu, Q., Yang, H., 2015. Short-term fidelity, habitat use and vertical movement behavior of the black rockfish *Sebastes schlegelii* as determined by acoustic telemetry. PLoS One 10 (8), e0134381. https://doi.org/10.1371/journal.pone.0134381.